Tectonophysics 708 (2017) 28–55

Contents lists available at ScienceDirect

Tectonophysics

journal homepage: www.elsevier.com/locate/tecto

Late Cretaceous to recent tectonic evolution of the North German Basin and the transition zone to the Baltic Shield/southwest Baltic Sea

M. Al Hseinat [a,b,*,1], C. Hübscher [a]

[a] Institute of Geophysics, Center for Earth System Research and Sustainability, University of Hamburg, Bundesstrasse 55, 20146 Hamburg, Germany
[b] Faculty of Marine Sciences, Department of Coastal Environment, the University of Jordan, PO Box 2595, Aqaba 77110, Jordan

ARTICLE INFO

Article history:
Received 9 November 2016
Received in revised form 6 March 2017
Accepted 19 April 2017
Available online 21 April 2017

Keywords:
Pleistocene tectonics
Recent tectonics
Ice-sheet loading
Glacial isostatic adjustment
Fault reactivation
Southwest Baltic Sea

ABSTRACT

In this study we investigate the Late Cretaceous to recent tectonic evolution of the southwestern Baltic Sea based on a dense grid of seismic reflection profiles. This area covers the Baltic Sea sector of the salt influenced North German Basin and its transition to the salt free Baltic Shield across the Tornquist Zone. The Upper Cretaceous to recent structural evolution is discussed by means of individual seismic sections and derived high-resolution time-structure maps of the main horizons, i.e., the Upper Cretaceous, Tertiary and Pleistocene. The Upper Cretaceous and Tertiary layers reveal numerous significant faults throughout the study area. Several of these faults propagate upwards across the unconsolidated Pleistocene sediments and occasionally penetrate the surface. The salt influenced North German Basin reveals three major fault trends: NW-SE, N-S and NNE-SSW. Several of these faults are located directly above basement (sub-salt) faults and salt pillows. The majority of these faults are trending N-S to NNE-SSW and parallel the direction of the Glückstadt Graben faults. In the salt free Tornquist Zone, we identify two major shallow fault trends, which are NW-SE and NE-SW. The majority of these faults are located above basement faults, following the direction of the Tornquist Zone. We conclude that generally basement tectonics controls activation and trends of shallow faults. If salt is present, the ductile salt layer causes a lateral shift between the sub- and supra-salt faults. Major plate reorganisation related to the Africa-Iberia-Europe convergence and the subsequent Alpine Orogeny caused reactivation of pre-existing faults and vertical salt movement in the Late Cretaceous. The change of stress orientation from NE-SW to a NW-SE during Neogene caused another phase of fault and salt tectonic reactivation. We explain that the ice-sheet loading and/or present-day stress field may have acted in combination, causing the recent tectonics and upward extension of the faults.

1. Introduction

The study area is located in the southwest Baltic Sea, covering the North German Basin and the transition zone to the Baltic Shield (Figs. 1 and 2a). Several marine geophysical studies carried out in the past decades have documented multiple tectonic events throughout the geological history of the region, for example the BABEL (BABEL working group, 1991, 1993), DEKORP-BASIN (e.g., DEKORP-BASIN Research Group, 1999; Krawczyk et al., 1999; Meissner and Krawczyk, 1999), EUGENO-S (EUGENO-S working group, 1998) and POLONAISE '97 (e.g., Grad et al., 1999; Guterch et al., 1999) projects. These projects mainly aimed on a better understanding of the deep-crustal structures therein. The overall tectonic evolution of the study area included five main periods, which are collision events during the Paleozoic, Permian rifting, extension during much of the Mesozoic, inversion during Late Cretaceous-Paleogene times and NW-SE extension since the Neogene. Repeated glaciation/deglaciation processes during Pleistocene times further had a significant impact on the evolution of northern Germany and surrounding areas (Reicherter et al., 2005). The advance and retreat of large ice sheets causes lithospheric depression and rebound in areas beneath and marginal to the ice, as the lithosphere equilibrate with the changing ice load (e.g., Sirocko et al., 2008).

This so called glacial isostatic adjustment (GIA) describes the response of the solid Earth to mass redistribution during a glacial cycle (e.g., Bergsten, 1954; Cathles, 1975; Ekman, 1991a, 1991b; Ekman, 2009; Ekman and Mäkinen, 1996; Johansson et al., 2002; Kaufmann and Wolf, 1999; Kierulf et al., 2014; Klemann and Wolf, 2005; Lambeck et al., 1998a; Mitrovica, 1996; Mörner, 1979; Plag et al., 1998; Spada et al., 2011; Steffen et al., 2006; Steffen and Wu, 2011; Whitehouse, 2009; Wolf, 1993; Wu and van der Wal, 2003). The

* Corresponding author at: Institute of Geophysics, Center for Earth System Research and Sustainability, University of Hamburg, Bundesstrasse 55, 20146 Hamburg, Germany.
E-mail addresses: muayyad.al-hseinat@uni-hamburg.de, m.hseinat@ju.edu.jo (M. Al Hseinat).
[1] Current address: Faculty of Marine Sciences, Department of Coastal Environment, the University of Jordan, Aqaba Branch, Jordan, PO Box 2595, Aqaba 77110, Jordan.

http://dx.doi.org/10.1016/j.tecto.2017.04.021
0040-1951/

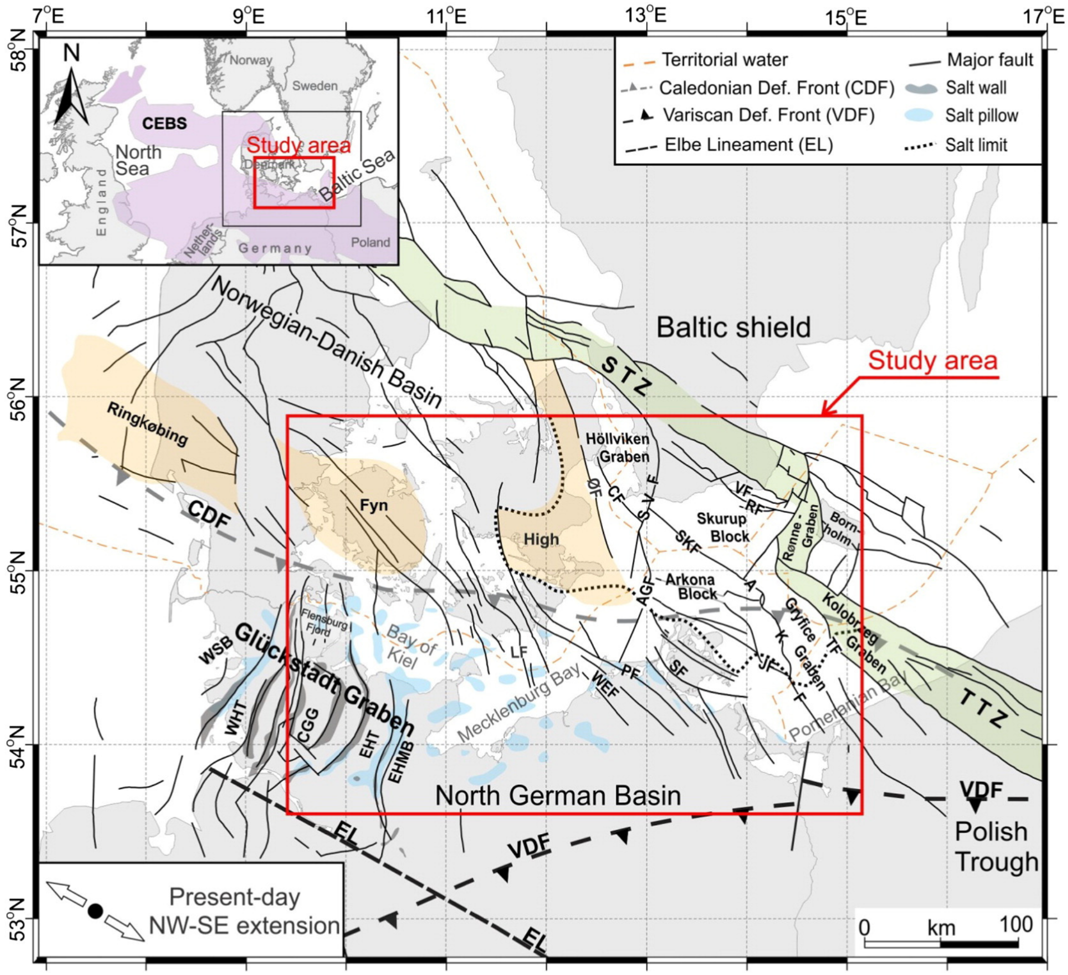

Fig. 1. Tectonic map of the Central European Basin System with the approximate location of the main structures within the study area (compiled from Baldschuhn et al., 1991; Bayer et al., 1999; Clausen and Pedersen, 1999; Krauss, 1994; Kossow et al., 2000; Lokhorst et al., 1998; Maystrenko et al., 2005a; NIA, 2000; Reicherter et al., 2008; Schlüter et al., 1997; Thomas et al., 1993; Vejbæk, 1997). The present-day stress field orientation is based on Kley et al. (2008) and Kley and Voigt (2008). AGF: Agricola Fault; AKF: Adler-Kamien Fault; CF: Carlsberg Fault; CGG: Central Glückstadt Graben; EHT: Eastholstein Trough; EHMB: Eastholstein Mecklenburg Trough; JF: Jasmund Fault; LF: Langeland Fault; ØF: Øresund Fault; PF: Prerow Fault; RF: Romeleasen Fault; SF: Samtens Fault; SKF: Skurup Fault; STZ: Sorgenfrei-Tornquist Zone; SVF: Svedala Fault; TF: Trzebiatow Fault; TTZ: Teisseyre-Tornquist Zone; VF: Vomb Fault; WEF: Werre Fault; WHT: Westholstein Trough; and WSB: Westschleswig Block.

rebound's influence of the last glacial advance is still happing and will continue for another few thousand years (e.g., Kumar and Sunil Singh, 2012; Le Meur, 1996; Steffen and Wu, 2011).

There is strong theoretical and empirical support for the idea that loading by major ice sheets does not only cause large-scale subsidence and lithospheric flexure, but also regional and local vertical and horizontal movements, which may be accommodated by faulting (e.g., Al Hseinat and Hübscher, 2014; Al Hseinat et al., 2016; Arvidsson, 1996; Brandes et al., 2012a, 2012b; Dyke et al., 1991; Fenton, 1994; Johnston, 1987; Kujansuu, 1964; Lagerbäck, 1978; Lagerbäck and Sundh, 2008; Lang et al., 2014; Muir-Wood, 2000; Munier and Fenton, 2004; Olesen, 1988; Quinlan, 1984; Sandersen and Jørgensen, 2015; Sauber and Molnia, 2004; Shilts et al., 1992; Steffen et al., 2014a, 2014b, 2014c, 2016; Stewart et al., 2000; Turpeinen et al., 2008; Wu et al., 1999). The effect of the ice loads on pre-existing faults and/or salt tectonics has been described in several studies (e.g., Al Hseinat and Hübscher, 2014; Al Hseinat et al., 2016; Brandes and Tanner, 2012; Lang et al., 2014; Lehné and Sirocko, 2007, 2010; Liszkowski, 1993; Sirocko et al., 2008; Stackebrandt, 2005). Reicherter et al. (2005) pointed out that the post-glacial landscape evolution in northern Germany shows significant fault reactivation.

Several geophysical studies in the western Baltic provided evidences for Tertiary tectonics, but the too low vertical resolution hampered studying shallow subsurface faulting and therewith recent tectonics (neotectonic) (e.g., Kossow and Krawczyk, 2002; Krawczyk et al., 2002; Krzywiec et al., 2003).

The availability of a large (~20.000 km) high-resolution, multi-channel seismic dataset collected between the Little Belt northwest of the Bay of Kiel and the Tornquist Zone provides the unique chance to close that gap (Fig. 2a). It adds valuable information to the understanding of the Late Cretaceous to recent structural evolution. The comparison of the Pleistocene faults map with deep-rooted faults will give a first idea about the driving forces, e.g., plate tectonics, salt tectonics or ice-load induced tectonics.

2. Tectonic evolution and main structural elements

Located along the northern margin of the Central European Basin System (CEBS) in the southwestern Baltic Sea, the study area has been long influenced by several major tectonic events from Paleozoic to present-day (Fig. 1). These include: the Caledonian and Variscan Orogenies (Late Cambrian-Late Carboniferous), rifting phases (Early Permian), subsidence during much of the Mesozoic, Late Cretaceous-Early Tertiary inversion and post-glacial isostatic adjustment since Late Pleistocene times.

During the Caledonian Orogen, the closure of the Tornquist Ocean was in the Ordovician-Silurian (Smit et al., 2016) resulting in accretion by oblique convergence and collision between Avalonia microcontinent

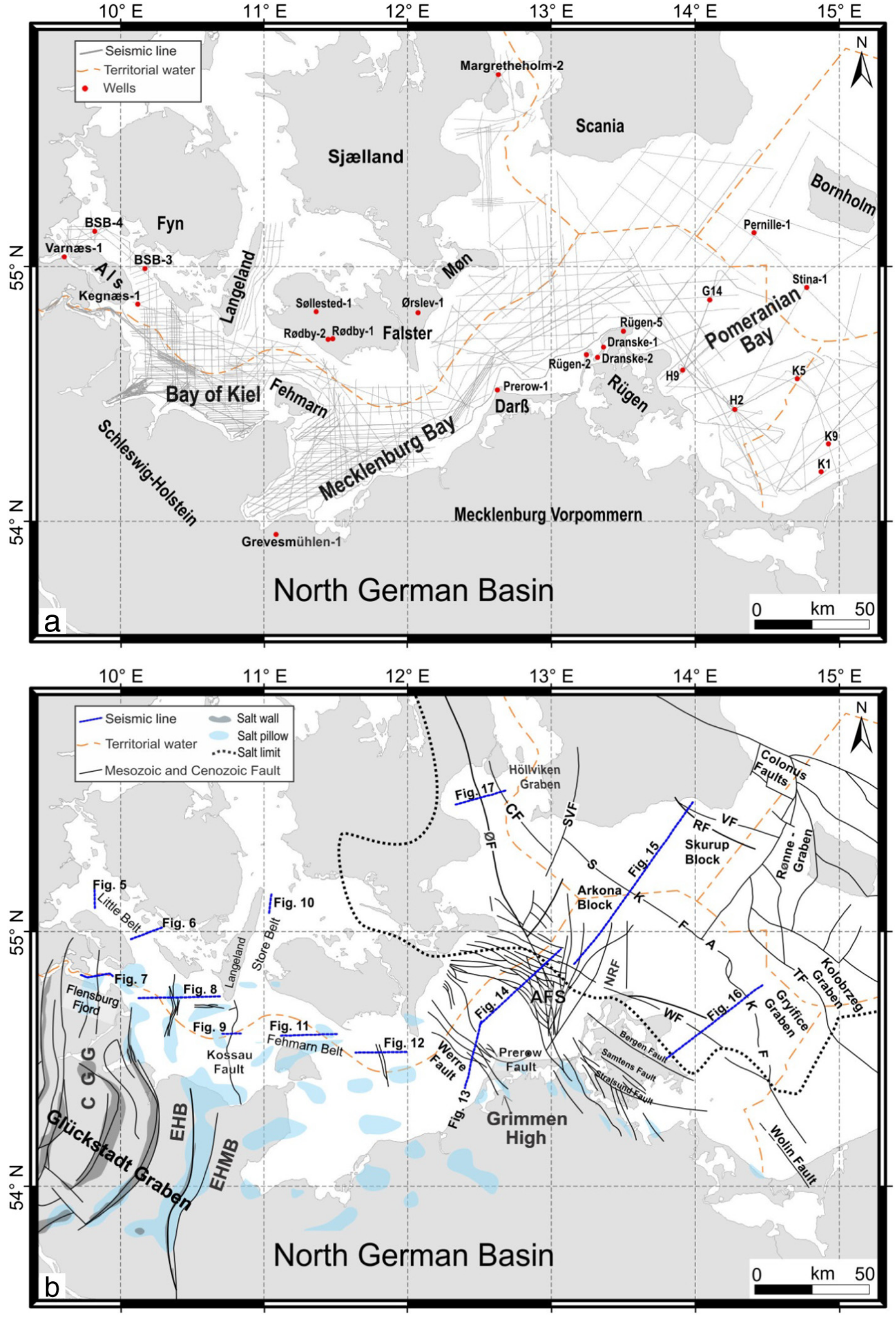

Fig. 2. Map of the study area (for location, see Fig. 1). (a) Shows the positions of the seismic sections as well as exploration and scientific wells. (b) Shows the distribution of salt walls and pillows (from Lokhorst et al., 1998), the locations of shown seismic profiles and Mesozoic-Cenozoic faults (compiled from Al Hseinat and Hübscher, 2014; Al Hseinat et al., 2016; Hansen et al., 2005; Bayer et al., 1999; Hübscher et al., 2010; Schlüter et al., 1997, 1998). AKF: Adler-Kamien Fault; CF: Carlsberg Fault; CGG: Central Glückstadt Graben; EHT: Eastholstein Trough; EHMB: Eastholstein Mecklenburg Trough; NRD: North Rügen Fault; ØF: Øresund Fault; RF: Romeleasen Fault; SVF: Svedala Fault; VF: Vomb Fault; and TF: Trzebiatow Fault.

and the Early Paleozoic passive margin of Baltica (Krawczyk et al., 2002). The prominent NW-SE striking Tornquist Zone is the longest pre-Alpine tectonic lineament of Europe and includes two segments, the Sorgenfrei-Tornquist Zone and Teisseyre-Tornquist Zone (Maystrenko et al., 2008). The Sorgenfrei-Tornquist Zone is considered as being the southwestern border of the Baltic Shield (Erlström et al., 1997; Gregersen et al., 2002, 2005; Shomali et al., 2006). The Teisseyre-Tornquist Zone separates Precambrian East European crust from Paleozoic crust of Central Europe (Berthelsen, 1992). During the Late Ordovician-Early Silurian, East Avalonia accreted to Baltica causing the formation of the Caledonian Deformation Front (Pharaoh et al., 1997), while Cocks et al. (1997) preferred the Elbe Lineament as the major contact zone. The Variscan Orogeny began towards the end of the Early Carboniferous and reached its maximum towards the end of the Late Carboniferous (Krauss, 1994). It consisted of compressional and extensional stress impulses, leading to an intensive fracture tectonic deformation of the Upper Devonian-Lower Carboniferous carbonate platform.

The Adler-Kamien Fault System is a thrust fault that is associated with the Teisseyre-Tornquist Zone. Based on the structure map of Bayer et al. (1999), the northern prolongation of this fault connects with the Skurup Fault, which is a NW-SE striking normal fault (Fig. 1). Both, the Adler-Kamien and Skurup Faults represent the transition from the Arkona Block to the Skurup Block (Fig. 1). The Adler-Kamien

Fault was originated by synsedimentary distensional faults of Permo-Carboniferous rift system and is presently active (Schlüter et al., 1998). The Skurup and Arkona Blocks (Fig. 1) constitute more or less horizontal uniform crustal blocks undisturbed by major faults (Erlström et al., 1997). The Agricola-Svedala Fault System represents the northwest border of this complex (Krauss, 1994). The formation of the Vomb Fault, Romeleasen Fault, Agricola-Svedala Fault System, North Rügen Fault, Rønne Graben and the southward half grabens, such as Gryfice Graben and Kolobrzeg Graben, result from an extensive phase related to Variscan tectonics (Figs. 1 and 2b: Krauss, 1994; Krauss and Mayer, 2004; Schlüter et al., 1998). According to Vejbaek (1985), the Rønne Graben is genetically comparable with the Höllviken Graben west of Scania; both were initiated by regional crustal extension causing subsidence of the Danish-Polish Trough in Late Carboniferous-Early Permian times. The Øresund Fault System is an extensional basement fault borders the Höllviken Graben (Fig. 1). The NNW-SSE trending Carlsberg Fault Zone is located east of the Ringkøbing-Fyn High and it is active at least since the break-up of Pangea in Triassic times (Kammann et al., 2016).

The NW-SE striking Trzebiatow Fault is a thrust fault, separating the Gryfice Graben in the west from the Kolobrzeg Graben in the east (Figs. 1 and 2b: Pokorski, 1990). The NW or NNW trending fault systems like Wiek Fault, Bergen Fault, Samtens Fault, Stralsund Fault, Prerow Fault or Werre Fault (Fig. 2b) are caused by the reactivation of pre-existing faults of the pre-Permian, Variscan and Caledonian basement during Triassic and Early Cretaceous times (Krauss and Mayer, 2004).

During the Early Permian times, a regional tectono-magmatic event developed accompanied by the main phase of thermal subsidence of the CEBS (Fig. 3; Kossow et al., 2000; van Wees et al., 2000). It is most likely responsible for the formation of the basement highs therein, such as the Ringkøbing-Fyn High (Cartwright, 1992). During the Early-Middle Permian times, nonmarine clastics (Rotliegend unit) were deposited across much of the North German Basin and the southwest Baltic region (Scheck and Bayer, 1999). Deposition of the Zechstein succession resulted from multiple marine transgressions from the north after a period of terrestrial conditions (Kossow et al., 2000; Taylor, 1998; Ziegler, 1990). This unit played a significant role during post-Permian times when the sedimentary infill of the sub-basins of the CEBS was strongly complicated by movements of Permian evaporate (Maystrenko et al., 2008). Three Permian-Mesozoic basins emerged in the study area: the North German Basin, the Norwegian-Danish Basin and the Polish Trough (Fig. 1). The Ringkøbing-Fyn High separates the North German Basin

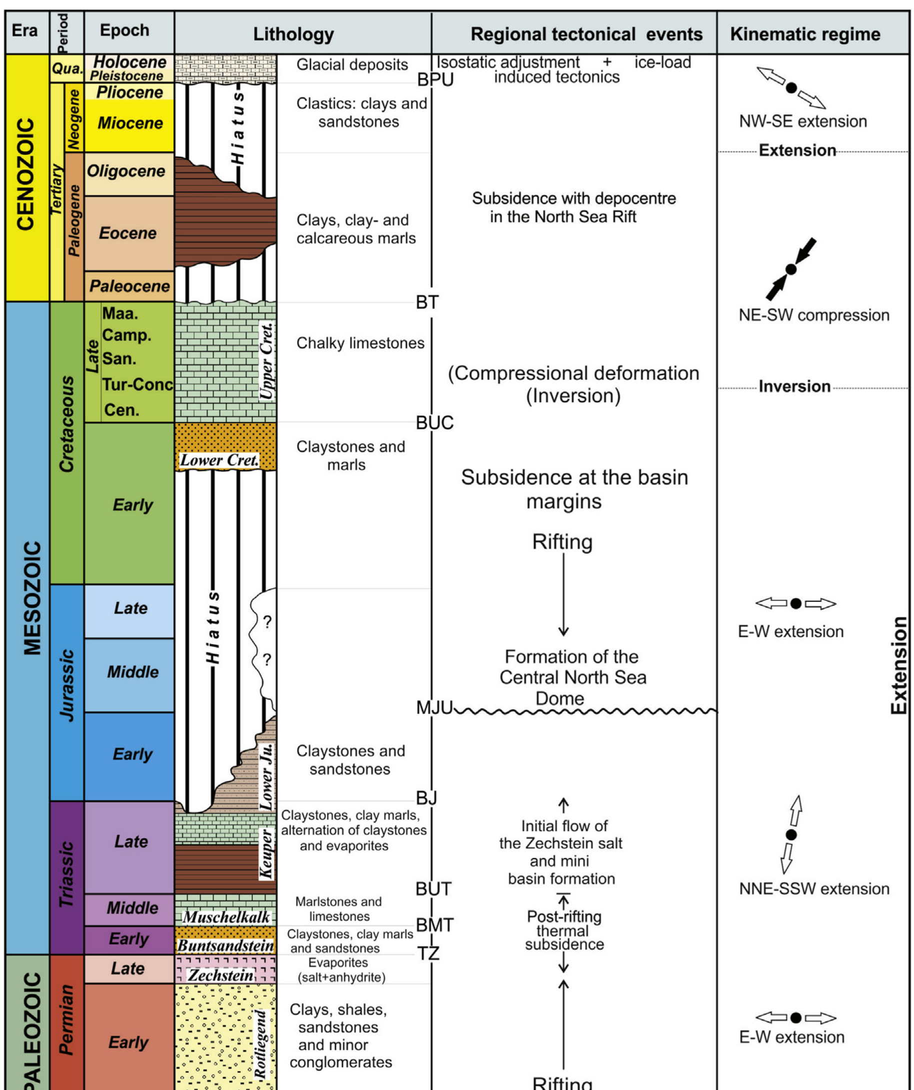

Fig. 3. Lithostratigraphic table (modified after Kossow et al., 2000) showing the dominant lithologies, main tectonic events and the ages of the major horizons interpreted along the northern margin of the North German Basin. Kinematic regime was summarized from Kley et al. (2008) and Kley and Voigt (2008). BJ: Base Jurassic; BMT: Base Middle Triassic; BPU: Base Pleistocene Unconformity; BT: Base Tertiary; BUC: Base Upper Cretaceous; BUT: Base Upper Triassic; MJU: Mid Jurassic Unconformity; and TZ: Top Zechstein.

from the Norwegian-Danish Basin in the southern North Sea across Denmark to Baltic Sea (Fig. 1; Cartwright, 1992; Clausen and Pedersen, 1999).

Several rifting phases affected much of northwest Europe, initiated in the Early Triassic period (Fig. 3; Ziegler, 1990). Subsidence continued throughout the Jurassic and Early Cretaceous times (Liboriussen et al., 1987). At the transition between the Middle and Late Triassic, a regional E–W directed extension created N-S trending depocentres, as well as the associated salt structures, such as the Glückstadt Graben (Figs. 1 and 2b). The Glückstadt Graben is one of the sedimentary basins where the sedimentary cover has been strongly affected by salt tectonics. It is subdivided into three main domains (Fig. 1): (i) the Central Glückstadt Graben; (ii) the marginal Eastholstein, Westholstein and Hamburg Troughs; and (iii) the outer Westschleswig and Eastholstein-Mecklenburg blocks at the Glückstadt Graben flanks (Maystrenko et al., 2008).

The development of the central North Sea Dome due to mantle plume activity caused a period of uplift and non-deposition during the Middle Jurassic to Early Cretaceous (Fig. 3; Underhill, 1998; Ziegler, 1990). This event led to the removal of parts of the Lower Jurassic and Upper Triassic successions in most parts of the study area (Kossow et al., 2000; Kossow and Krawczyk, 2002; Scheck et al., 2003a). Rifting during the latest Middle Jurassic to Late Jurassic resulted in reactivation of the sub-basins-bounding fault systems, supra-salt faulting and further growth in salt structures (Maystrenko et al., 2011). These authors pointed out that the eastern SW–NE trending marginal Eastholstein Trough evolved during this rifting phase. Based on Al Hseinat and Hübscher (2014), the almost N-S striking Kossau Fault within the Bay of Kiel represents a north prolongation of the Eastholstein Mecklenburg Block (Fig. 2b).

Sediment deposition associated with slow (thermal) subsidence resumed at the end of the Early Cretaceous (Albian) and continued without major tectonic activity until the Late Cretaceous (Fig. 3; Ziegler, 1990). In the latest Cretaceous Africa-Iberia-Europe collided, causing the formation of the Alpine Orogen (Kley and Voigt, 2008; Krauss, 1994; Maystrenko et al., 2008; Thybo, 2001; Ziegler, 1990). The collision-induced compressional stresses affected the whole Europe. Some basins underwent contraction and inversion like the Subhercynian Basin at the southern margin of the CEBS (Brandes et al., 2013; Stackebrandt, 1986; Voigt et al., 2006; von Eynatten et al., 2008). In contrast to other basins of the CEBS, the Glückstadt Graben was essentially not inverted (Grassmann et al., 2005; Maystrenko et al., 2005a), with upward salt movement (Bayer et al., 1999; Kley and Voigt, 2008; Krauss, 1994; Scheck-Wenderoth and Lamarche, 2005; Ziegler, 1990). While the basement controlled Grimmen High was inverted with uplift values up to 500 m (Fig. 2b; Kossow et al., 2000). The Tornquist Zone and adjoining faults were reactivated and inverted accordingly (Kley and Voigt, 2008; Maystrenko et al., 2008; Thybo, 2001). As summarized by Kley et al. (2008), the kinematics in the Neogene are quite complex. Between the Late Eocene and Middle Miocene in the North German Basin (Figs.1 and 2b), the principal horizontal stress orientation changed from a NE-SW to a NW-SE, the present-day orientation, and oblique to the Glückstadt Graben (Grassmann et al., 2005; Kley et al., 2008). Kaiser et al. (2005) calculated actual slip rate of ~0.014 mm/a for this graben.

The analysis of the time-isochore maps of post-Permian strata in the Bays of Kiel and Mecklenburg suggested a causative correlation between tectonic evolution of the North German Basin and halokinetics (Hansen et al., 2005; Hübscher et al., 2010). In contrast to the salt pillows which emerged above Triassic fault systems in the Bay of Kiel, the Cenozoic salt movement activity is most pronounced in the Bay of Mecklenburg (Hübscher et al., 2010). Similar study focusing on the pre-Alpine evolution have been carried out in the Bay of Mecklenburg by Zöllner et al. (2008), based on a very dense reflection seismic profile grid. Tertiary to recent halokinetics and faulting in the supra-Zechstein succession in the southwest Baltic Sea are due to the Neogene to recent NW-SE directed extension, the present-day orientation (Figs. 1 and 3; Al Hseinat and Hübscher, 2014; Al Hseinat et al., 2016).

Since the mid-Quaternary times, the study area and adjacent areas have experienced at least three extensive glaciations: the Elsterian, Saalian and Weichselian ice sheets (Fig. 4; Ehlers et al., 2011; Hughes et al., 2016; Roskosch et al., 2015). During the last glacial maximum, the Weichselian ice sheet covered eastern and northern Denmark, northeastern Germany, northern Poland and northern Britain (Fig. 4; Bowen et al., 1986; Cameron et al., 1987; Ehlers and Wingfield, 1991; Long et al., 1988; Pasierbski, 1979). The ice movement direction was approximately perpendicular to the present shoreline of the Baltic Sea Basin (Fig. 4; Piotrowski, 1997; Piotrowski and Tulaczyk, 1999). Since the last deglaciation, the development of the entire Baltic Basin has been closely related to balance between eustatic sea-level rise and isostatic uplift of the Fennoscandia (Lemke et al., 1994). The decay of the ice sheets is likely to have changed the equilibrium situation in the crust and upper mantle (Sirocko et al., 2008). The elastic response to the temporal and spatial varying ice-loads is considered to be instantaneous, whereas the viscoelastic response of the mantle is much slower and is active even thousands of years after the ice retreat (Stewart et al., 2000). These authors showed how the ice sheet loading/unloading may modulate not only the deep-seated viscoelastic response of the Earth, but also the nature and incidence of upper-crustal faulting, in addition to earthquake generation. Based on seismic data, Brandes et al. (2011) developed a tectonic model showing the reactivation of basement faults as a consequence of ice sheet loading. Brandes et al. (2011) also pointed out that the advancing ice sheet caused far field extensions within northwestern Germany, which might have reactivated the pre-existing normal faults.

Recent fault movements are still being recorded in the CEBS and the southwest Baltic Sea (e.g., Al Hseinat and Hübscher, 2014; Al Hseinat et al., 2016; Brandes et al., 2011; Brandes et al., 2012a; Brandes et al., 2015; Cloetingh et al., 2005; Kammann et al., 2016; Lehné and Sirocko, 2010; Ludwig, 1995). These authors stated that the deformation was most likely caused by an ongoing glacial isostatic adjustment since time of the Late Pleistocene Weichselian maximum.

3. Database

3.1. High-resolution multi-channel seismic

During 1998–2004, the Universities of Aarhus and Hamburg collected parts of the high-resolution multi-channel seismic sections used in this study as part of the BaltSeis and NeoBaltic projects (Fig. 2a; Hansen et al., 2005, 2007; Hübscher et al., 2004, 2010). Further reflection seismic sections were collected during multiple student field exercises of the University of Hamburg between 2005 and 2014. Seismic sections cover large scale area within the southwest Baltic Sea, mostly between the Bay of Kiel and the Tornquist Zone with a total length of ~20.000 km. For a general description of the marine seismic method see Hübscher and Gohl (2014).

The seismic data acquisitions were completed with different sources on the different surveys, i.e. the airgun and sparker sources. For the airgun seismics, a sleeve-gun cluster consisting of four synchronized guns with a total volume of 1.1 l, pressured at 100 bar or a single GI-gun with a 0.7 l Generator and a 1.7 l Injector chamber volume were used. The dominant frequency of these sources is ~100 Hz. The active length of the seismic cable was 100–600 m. Analog streamer data were recorded digitally with a sample interval of 1 ms. The overall good penetration lies in between 1.5 s and 2 s two-way travel time (TWT). Vertical stratigraphic resolution of the seismic data is between 8 and 10 m whereas the horizontal resolution is in the order of 20–25 m. For the sparker seismics, three electrode pairs with distances of ~1.2 m were fired with 1800 kJ. The main signal frequency was ~250 Hz and the sample rate was 0.5 ms. All data were post-stack time migrated.

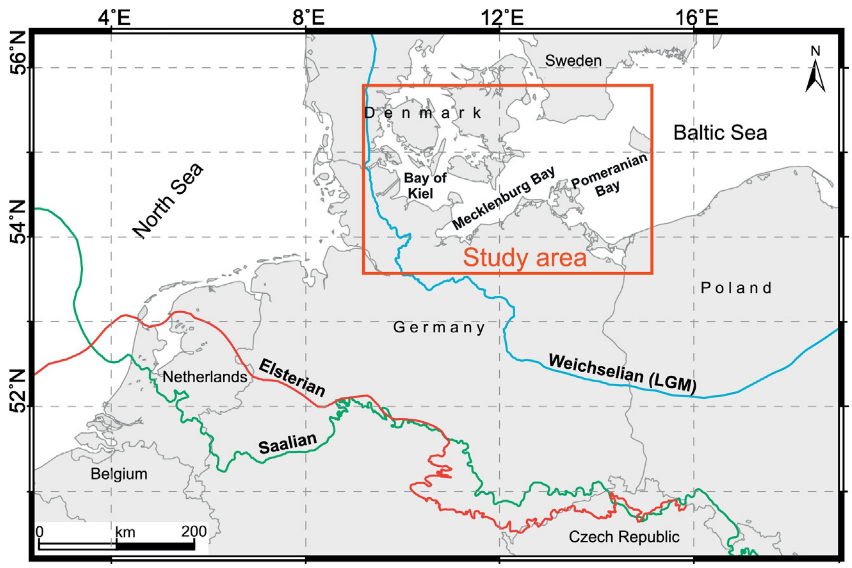

Fig. 4. Approximate maximum extent of the Middle and Late Pleistocene ice sheets (modified after Ehlers et al., 2011; Hughes et al., 2016; Roskosch et al., 2015).

Amplitude losses were compensated by a power function of TWT, which gradually enhanced reflection amplitudes with travel time. The post-stack time migrated seismic data were uploaded to the IHS "Kingdom" interpretation system for structural interpretation. The vertical exaggeration (VE) in the shown seismic data is calculated with a constant interval velocity of 1500 m/s.

3.2. Well data correlation

Several exploration and scientific wells were correlating the different interpreted horizons on the seismic profiles (Fig. 2a). The exploration wells include: (i) Danish wells; the onshore Varnæs-1, Søllested-1, Ørslev-1, Rødby-1 and Rødby-2 (Nielsen and Japsen, 1991) and the offshore Kegnæs-1 (Gearhart Geo Consultants, 1985), Margretheholm-2 (Dong Efterforskning og Production, 2003), Pernille-1 and Stina-1 (Schlüter et al., 1997); (ii) German wells; the onshore Grevesmühlen-1, Prerow-1, Dranske-1, Dranske-2, Rügen-2 and Rügen-5 (Hoth et al., 1993) and the offshore H2, H9, G14 and K5 (Schlüter et al., 1997); and (iii) Polish wells; K1 and K9 (Schlüter et al., 1997). The scientific wells include the Danish wells; BSB-3 and BSB-4 (Andren et al., 2012).

3.3. Seismo-stratigraphic framework

The seismo-stratigraphic description is mainly based on previous studies by Hansen et al. (2005, 2007), Hübscher et al. (2010) and Lykke-Andersen and Surlyk (2004). Additional seismic lines were also measured strategically nearby well sitesto obtain a better stratigraphic calibration (Fig. 2a). The signal-noise ratio allowed identifying the following major seismic stratigraphic units across the entire southwest Baltic Sea: Lower Triassic (Buntsandstein), Middle Triassic (Muschelkalk), Upper Triassic (Keuper), Jurassic, Lower Cretaceous, Upper Cretaceous (Base Chalk Group), Tertiary, Pleistocene and, locally, Holocene. The successions are bound by prominent unconformities and their correlative conformities include: the Base Middle Triassic; BMT, Base Upper Triassic; BUT, Base Jurassic; BJ, Mid Jurassic Unconformity; MJU, Base Upper Cretaceous; BUC, Base Tertiary; BT, Base Quaternary Unconformity (here: Base Pleistocene Unconformity; BPU) and the seafloor horizon (Figs. 5–17). The Top Zechstein surface (Base Lower Triassic) is traceable on only a few seismic sections (e.g., Fig. 8). We used the following interval velocities of Hansen et al. (2007) for the calculation of fault displacements: Pleistocene: 1800 m/s, Tertiary: 2000 m/s, Cretaceous: 2400 m/s, Jurassic-Upper Triassic: 2600 m/s and Middle Triassic: 3500 m/s. Seafloor depths were corrected with a constant interval velocity of 1500 m/s.

The angular unconformity (MJU) at depths between 600 m and 1200 m separates the Cretaceous and Cenozoic sediments from older strata (Figs. 5–17). It corresponds with the major transgression of Albian age from non-deposition to shallow marine conditions (Gearhart Geo Consultants, 1985; Kossow et al., 2000). Hübscher et al. (2010) described the same unconformity within the Mecklenburg Bay as the Base Cretaceous Unconformity. The BUC horizon is the well traceable Base Cenomanian reflection close to the top of the Albian transgression (MJU).

The MJU and BUC horizons mark the base and the top of the Lower Cretaceous unit, respectively (Figs. 5–17). The succession consists of calcareous sediments, primarily red marls (Scheck and Bayer, 1999). This unit represents a thin succession of uniform thickness of ~48 m (40 ms TWT), traceable over the entire study area.

The Upper Cretaceous unit overlies the BUC horizon and is at the top bounded by the BT horizon northwest of the North German Basin (Figs. 5–12) and by the BPU reflection northeast of it (Figs. 13–17). The unit consists mainly of chalk sediments deposited during shallow marine becoming open marine conditions (Scheck and Bayer, 1999). Several parallel internal reflections (IUC1 and 2) can, however, be seen within this unit (Figs. 8–14). Based on comparison to H2 and H9 exploration wells (Schlüter et al., 1997), it was possible to identify the Base Santonian and Base Maastrichtian horizons within the eastern part of the study area (Figs. 15 and 16).

The Tertiary unit overlies the BT horizon and extends upwards to the BPU reflection (Figs. 5–12). The unit consists mainly of brackish marine clay-silt sediments (Scheck and Bayer, 1999). Two internal reflections (IT1 and 2) are another characteristic of this succession (e.g., Fig. 9).

In the entire study area, the BPU represents an onlap or downlap surface which truncates the underlying Tertiary deposits (e.g., Fig. 8). This erosional surface formed during Pleistocene times. The limited vertical resolution of the seismic data hampers the identification of Holocene strata in most regions with the exception of the Little Belt.

4. Time-structure and time-isochore maps

4.1. Methods

All profiles shown in Fig. 2a were used for the mapping procedure. The time-structure maps show the present-day vertical depth in TWT

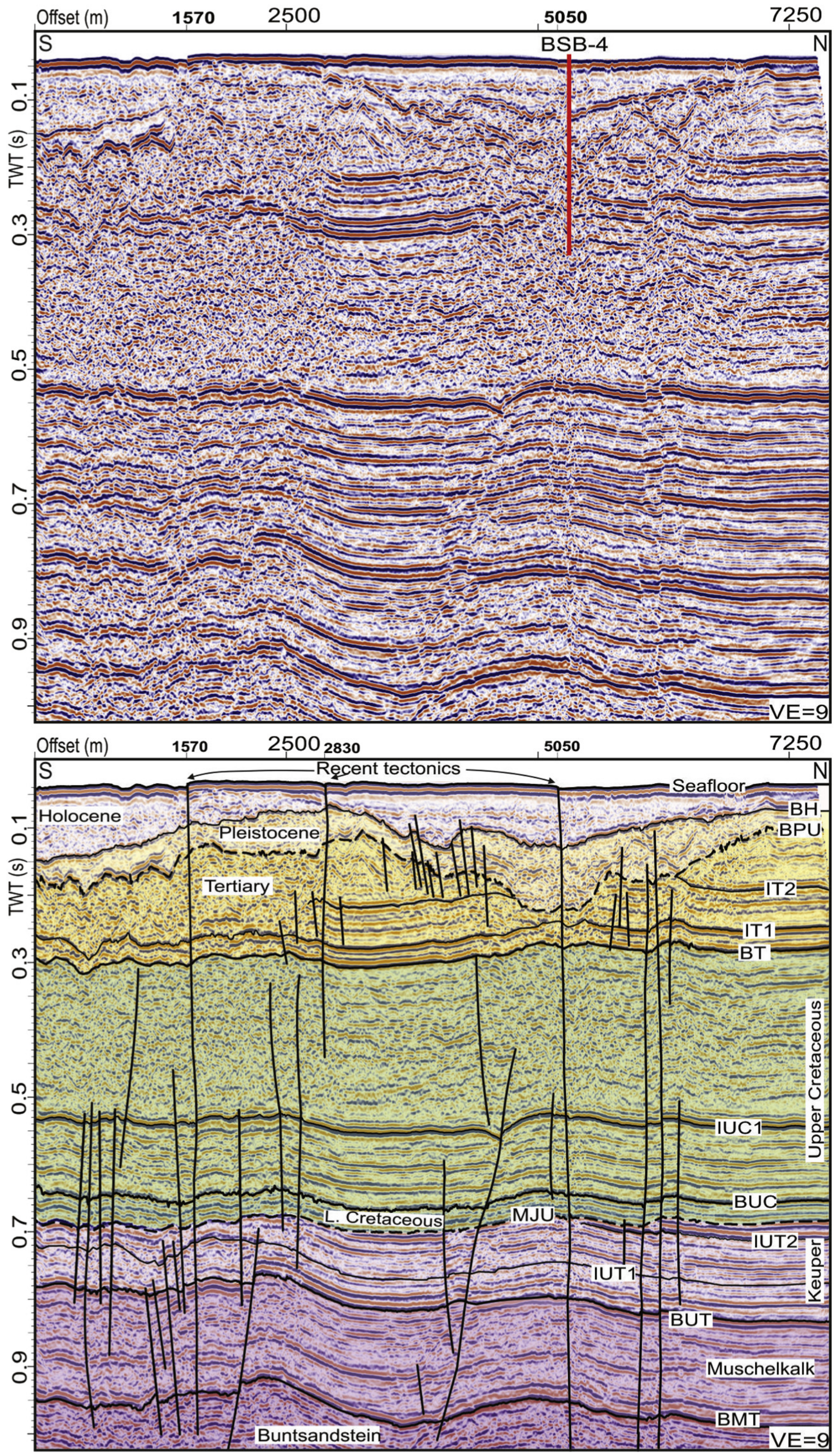

Fig. 5. S-N time-migrated seismic section (for location, see Fig. 2b) and interpreted section in northern prolongation of the Central Glückstadt Graben. Two major faults are cutting the strata from Triassic into the Holocene deposits. These faults penetrate the seafloor horizon. Black lines mark fault systems. BH: Base Holocene; BMT: Base Middle Triassic; BPU: Base Pleistocene Unconformity; BT: Base Tertiary; BUC: Base Upper Cretaceous; BUT: Base Upper Triassic; IUC 1: Internal Upper Cretaceous 1; IUT 1 and 2: Internal Upper Triassic 1 and 2; IT 1 and 2: Internal Tertiary 1 and 2; and MJU: Mid Jurassic Unconformity.

to the specific surfaces, i.e., the BUC, BT and the BPU (Figs. 18–20). These maps allow identifying the locations and trends of different fault systems that cut the above-mentioned surfaces. Only faults that can be traced from line to line across the survey have been included into the time-structure maps. The time-isochore map in Fig. 21 shows the present-day vertical time-interval in TWT of the Pleistocene unit, bounded by the BPU horizon (base) and seafloor (top). This map allows the discussion of thickness variations of the Pleistocene deposits throughout the southwest Baltic Sea. Due to shallow water depth and the combined interpretation of several datasets, which have been collected with different streamers and seismic sources, the TWT of the seafloor reflection was not always consistent with the detailed bathymetry grid of Seifert et al. (2001) (Fig. 22). Miss-ties between different profiles resulted, e.g., from streamer static or inaccurate determined distances

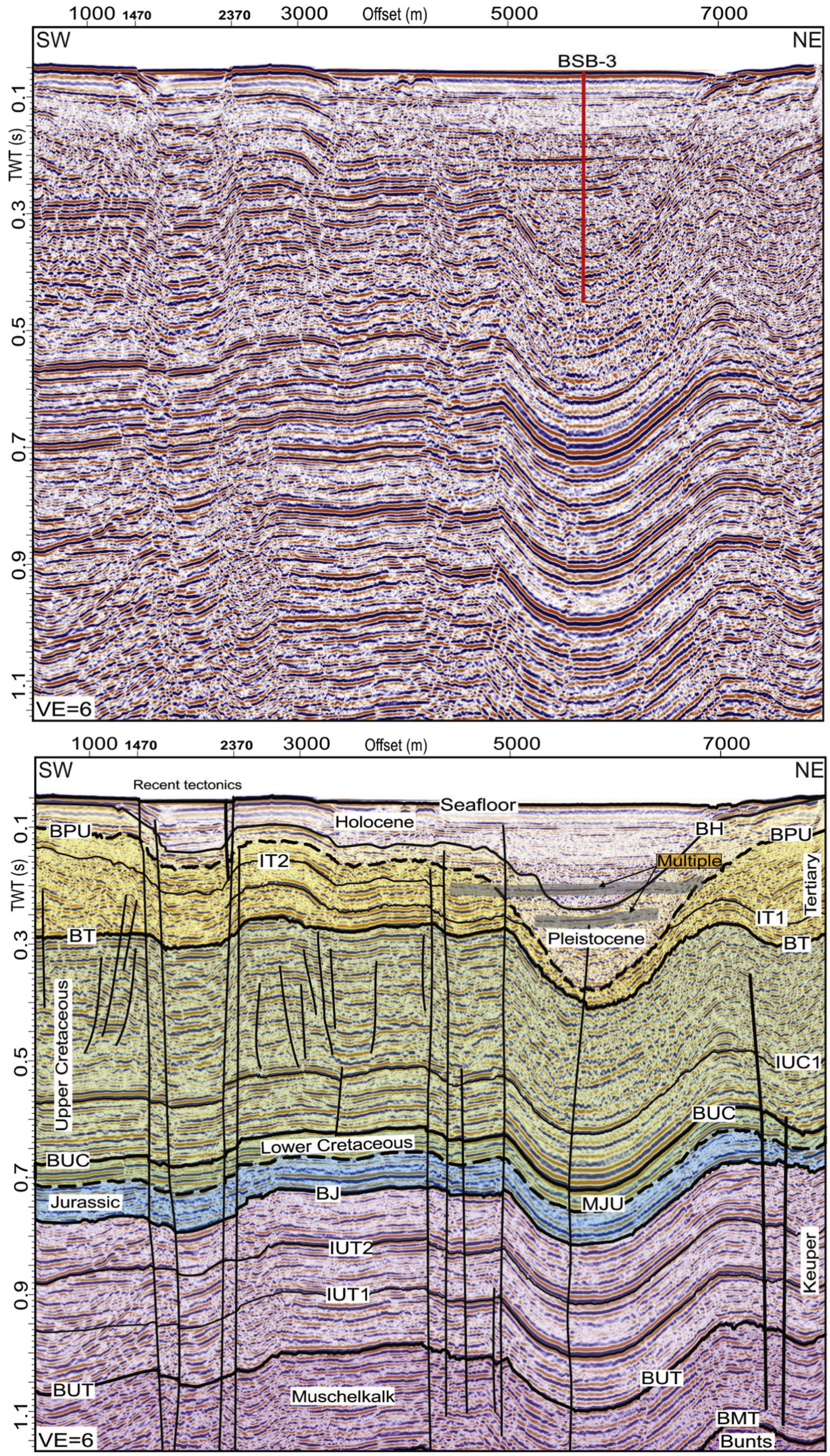

Fig. 6. SW-NE time-migrated seismic section (for location, see Fig. 2b) and interpreted section north of the marginal Eastholstein Trough. Several normal faults cut the entire succession. From the western part, some of these faults intersect the BPU horizon and propagate upwards into the seafloor horizon. The seafloor horizon falls down between these faults. Black lines mark fault systems. BH: Base Holocene; BJ: Base Jurassic; BMT: Base Middle Triassic; BPU: Base Pleistocene Unconformity; BT: Base Tertiary; BUC: Base Upper Cretaceous; BUT: Base Upper Triassic; IUC 1: Internal Upper Cretaceous 1; IT 1 and 2: Internal Tertiary 1 and 2; IUT 1 and 2: Internal Upper Triassic 1 and 2; and MJU: Mid Jurassic Unconformity.

between the seismic source and the hydrophone groups. In order to overcome these inaccuracies, we converted the bathymetry into a time-structure map (measured in TWT) by using a constant interval velocity of 1500 m/s. The time-structure map of the Base Pleistocene has been calculated by subtracting the TWT interval between seafloor and BPU reflections from the TWT corrected bathymetry (Fig. 20). The corrected Pleistocene time-isochore map (Fig. 21) was produced by adding the TWT converted bathymetry to the corrected Base Pleistocene time-structure map.

Afterwards, the time-structure and time-isochore grids were exported and re-gridded in ArcMap (ESRI version 10.0) allowing a better interpolation between different seismic lines and to enhance the resolution of the final output images. For all grids, Ordinary-Kriging interpolation method with 100 m cell size was applied. A 50 ms contour

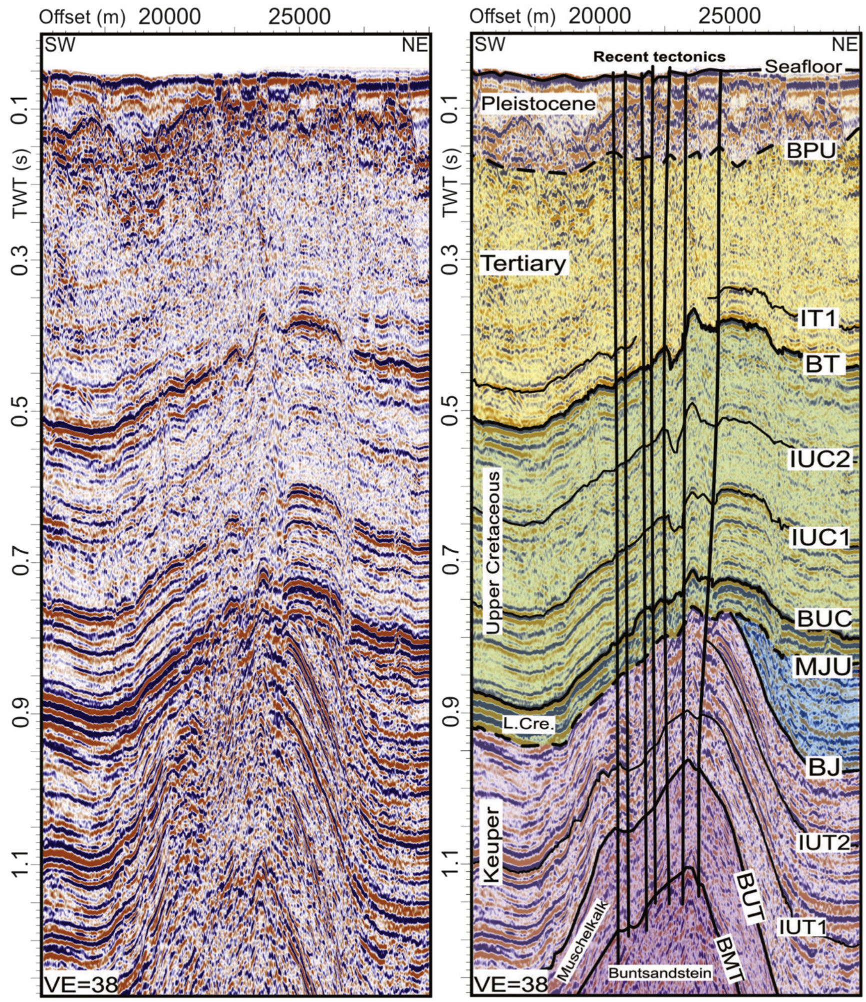

Fig. 7. SW-NE time-migrated seismic section (for location, see Fig. 2b) and interpreted section crossing the N-S sub-salt fault related to the Central Glückstadt Graben. An anticline structure above the Zechstein salt is observed. Within the central anticline, a set of normal faults cut the entire succession. Seafloor topography is cut by faulting. Black lines mark fault systems. BJ: Base Jurassic; BMT: Base Middle Triassic; BPU: Base Pleistocene Unconformity; BT: Base Tertiary; BUC: Base Upper Cretaceous; BUT: Base Upper Triassic; IUC 1 and 2: Internal Upper Cretaceous 1 and 2; IT 1: Internal Tertiary 1; IUT 1 and 2: Internal Upper Triassic 1 and 2; and MJU: Mid Jurassic Unconformity.

interval was used for both, the Base Cretaceous and the Base Tertiary time-structure maps while a 25 ms contour interval was used for the Pleistocene time-structure and time-isochore maps. The outer boundaries of the maps have been constrained by data coverage and seismic profiles running along the 10 m isobaths close to the northern coasts of Germany.

4.2. Observations

The Lower and Upper Cretaceous sediments are present throughout the entire study area (Figs. 5–17). Assuming an average interval velocity of the Cretaceous of 2400 m/s (Hansen et al., 2007), the Lower Cretaceous succession shows a more or less constant thickness of ~48 m. Hence, no correlation of this layer was carried out using seismic interpretation of this study. The time-structure map of the BUC surface (Fig. 18) shows an increasing depth of the layer towards the North German Basin, particularly in the Bays of Eckernförde and Mecklenburg. Major and minor topographic highs are observed above the salt pillows within the Bays of Kiel and Mecklenburg (Fig. 18). It is seen that they are more pronounced in the Mecklenburg Bay. In general, the shallowest parts of these sediments are observed north of the Grimmen High and within the Pomeranian Bay.

Tertiary sediments are only preserved north-west of the North German Basin (Fig. 19). The maximum depth of the BT reflection ranges between ~64 m and 1180 m. It generally deepens towards the centre of the North German Basin in the south. Like the previously described Upper Cretaceous succession, several major and minor topographic highs are observed above salt pillows within the Bays of Kiel and Mecklenburg and they are more pronounced within the Mecklenburg Bay (Fig. 19).

Pleistocene sediments are present in the entire study region (Fig. 20). The maximum depth of the BPU horizon is ranging between ~18 m and 32 m. Seismic data interpretations show that the BPU surface was affected by glacial erosion during Pleistocene times (e.g., Figs. 8 and 9). The BPU time-structure map exhibits several topographic lows marked "a-g" in Fig. 20: (a) the BPU reveals high depth values in the Little Belt between Als and Fyn Islands; (b) marks a N-S trending erosional valley corresponds to the interpreted valley in Fig. 8; (c) shows an elongated topographic low corresponds with the Kossau tunnel valley (Fig. 9) described by Al Hseinat and Hübscher (2014); (d) shows an *E*-W striking topographic low in Fehmarn Belt; (e) here, an E-W trending erosional valley in the central Mecklenburg Bay could be mapped over a length of ~17 km; (f) marks a SW-NE directed minor topographic low northeast of DarßIsland could be mapped over a distance of 34 km described by Lemke et al. (1994); and (g) marks the Arkona Basin northeast of Rügen Island.

The time-isochore map (Fig. 21) gives a volumetric estimation of the Pleistocene sediments in the entire southwest Baltic Sea. It is generally a thin succession with a thickness ranging between ~1 m and 280 m. This

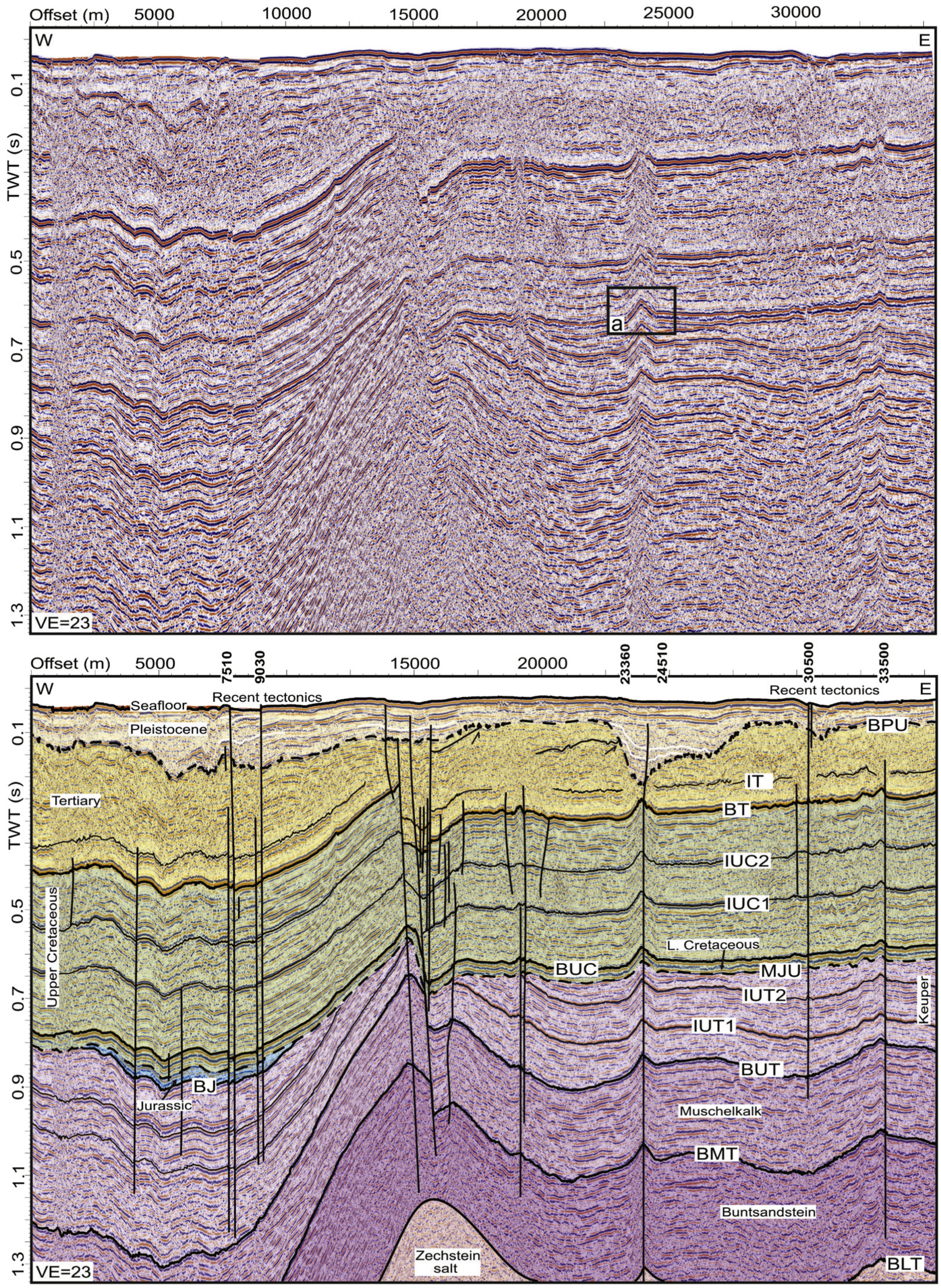

Fig. 8. W-E time-migrated seismic section (for location, see Fig. 2b) and interpreted seismic section running through the northwest part of the Bay of Kiel. The section crosses a NW-SE striking sub-salt basement fault. The entire post-Permian succession reveals anticline between offsets 23,358 m and 24,510 m. A deep erosional valley is observed above the anticline. A near-vertical fault cuts throughout the anticline from Zechstein into the Pleistocene deposits. Several faults are cutting the entire succession at least from Muschelkalk into the Pleistocene deposits. Some of them even pierce the seafloor. Black lines mark fault systems. BJ: Base Jurassic; BLT: Base Lower Triassic; BMT: Base Middle Triassic; BPU: Base Pleistocene Unconformity; BT: Base Tertiary; BUC: Base Upper Cretaceous; BUT: Base Upper Triassic; IUC 1 and 2: Internal Upper Cretaceous 1 and 2; IT: Internal Tertiary; IUT 1 and 2: Internal Upper Triassic 1 and 2; and MJU: Mid Jurassic Unconformity.

map also shows several major and minor anomalies marked "a-g" in Fig. 21: (a) major anomalies in the Little Belt between Als and Fyn Islands; (b) high anomalies along the erosional valley shown in Fig. 8; (c) high anomalies along the Kossau tunnel valley; (d) minor anomalies in Fehmarn Belt; (e) high anomalies within the erosional valley in the central Mecklenburg Bay; (f) minor anomalies with ~48–60 m thick corresponds to the tunnel valley northeast Darß Island; and (g) marks minor anomalies within the Arkona Basin northeast of Rügen Island.

5. Structural style

In the following, we briefly describe the several fault systems. Details as length of the fault systems, fault offsets etc. are summarized in Table 1.

5.1. Fault systems

The seismic section in Fig. 5 runs S-N in the Little Belt and therewith parallel to the northern prolongation of the Central Glückstadt Graben

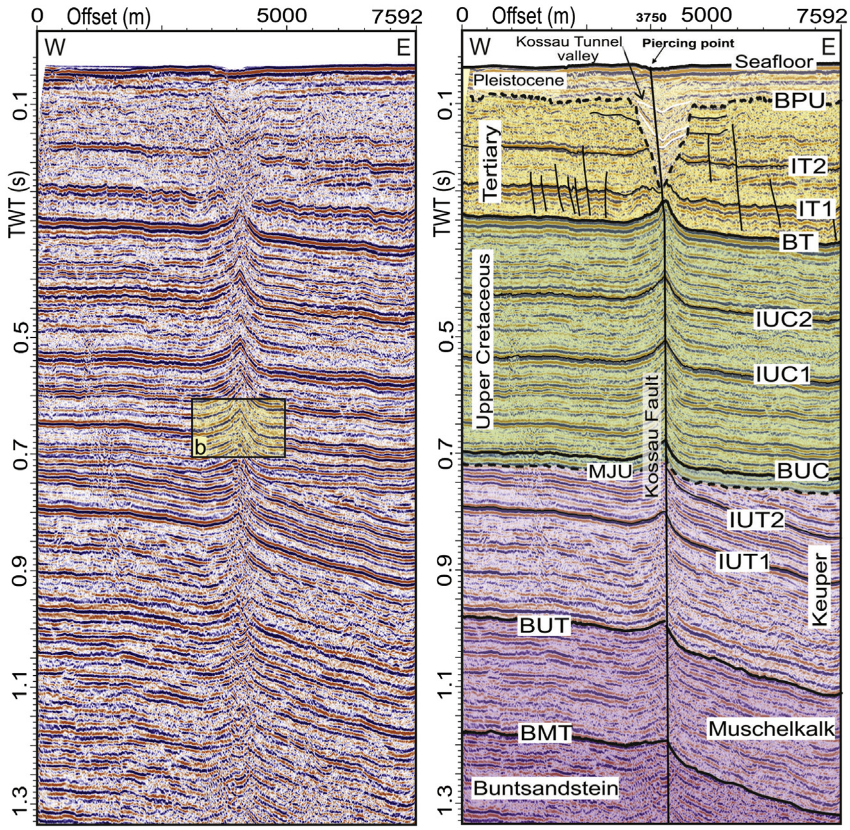

Fig. 9. W-E time-migrated seismic section (for location, see Fig. 2b) and interpreted section crossing the S-N striking Kossau Fault. The entire post-Permian succession reveals anticline. A deep erosional valley (Kossau Tunnel valley) is observed directly above the anticline. The Kossau fault cuts the strata from Triassic into the Pleistocene deposits. It is also piercing the seafloor horizon. Black lines mark fault systems. BJ: Base Jurassic; BMT: Base Middle Triassic; BPU: Base Pleistocene Unconformity; BT: Base Tertiary; BUC: Base Upper Cretaceous; BUT: Base Upper Triassic; IUC 1 and 2: Internal Upper Cretaceous 1 and 2; IT 1 and 2: Internal Tertiary 1 and 2; IUT 1 and 2: Internal Upper Triassic 1 and 2; and MJU: Mid Jurassic Unconformity.

(Fig. 2b). It shows two near-vertical faults cutting the entire succession from Triassic up to the seafloor. At offset 2830 m, a normal fault cuts the upper part of the Upper Cretaceous across the Pleistocene and propagates up to the seafloor (Fig. 5). Several other normal and near-vertical faults cut the BUC, BT and BPU surfaces.

Further east in the Little Belt, the seismic profile in Fig. 6 strikes SW-NE north of the marginal Eastholstein Trough (Fig. 2b). It shows a set of normal and near-vertical faults cut through the post-Permian succession. Four of them even intersect the BPU horizon and reach upwards into the Holocene deposits.

The SW-NE seismic section (Fig. 7) crosses the almost N-S striking sub-salt basement fault of the Central Glückstadt Graben in the Flensburg Fjord (Figs. 1 and 2b). The entire post-Permian succession forms an anticline above the Zechstein salt pillow. A set of normal faults cut through the entire supra-salt succession from Triassic rocks across the Pleistocene deposits and pierce the seafloor.

In Fig. 8, the seismic section runs W-E and crosses a salt pillow that emerged above a NW-SE striking sub-salt basement fault (Figs. 1 and 2b). At offset 15,000 m, several supra-salt normal faults cut the succession above the Zechstein pillow (Fig. 8). Two of them reach upwards across the Pleistocene deposits and pierce the seafloor. Furthermore, at offsets 30,500 m and 33,500 m two normal faults dissect the succession from the Triassic strata into the Tertiary deposits. One of them reaches at least from Muschelkalk into the Pleistocene sediments and pierces the seafloor.

The W-E seismic profile in Fig. 9 crosses the N-S to NNE-SSW striking Kossau Fault (Fig. 2b), which has been interpreted as the northward prolongation of the marginal Eastholstein Mecklenburg Block by Al Hseinat and Hübscher (2014). An anticline of <2000 m in width underlies an erosional valley, referred to as the Kossau Tunnel valley (Atzler, 1995).

North of the Caledonian Deformation Front (Fig. 1), the seismic section in Fig. 10 runs SSW-NNE northeast of the Langeland Island within the Store Belt (Fig. 2b). Between offsets 44,000 m and 47,000 m, two conjugate normal faults cut the strata from Triassic into the Pleistocene, causing a graben structure. Both are growth faults. Within the central graben, a set of normal faults cut the upper part of the Upper Cretaceous succession into the Tertiary sediments. One of these faults reaches upwards across the Pleistocene deposits penetrating the seafloor horizon. Several normal faults occur in both sides of the graben within the Triassic sediments. At offset 43,000 m, other normal fault intersects the entire succession at least from Muschelkalk into the Tertiary deposits.

Near the north-eastern margin of the North German Basin within the Fehmarn Belt, the seismic profile in Fig. 11 runs W-E and crosses a salt pillow that emerged above a NW-SE striking sub-salt basement fault (Figs. 1 and 2b). Between offsets 18,500 m and 22,500 m, the entire post-Permian succession reveals two V-shape anticlines with a width of ~800 m. Within these anticlines, the TWT interval of the reflections decreases slightly with depth. In the centre of each anticline, a fault cuts through the entire succession at least from Muschelkalk into the Tertiary sediments.

Near the northern margin of the North German Basin, the seismic section shown in Fig. 12 runs W-E and crosses the NW-SE striking Langeland Fault described by Baldschuhn et al. (1996) and NIA (2000) (Figs. 1 and 2b). Between offsets 23,000 m and 27,500 m, this section shows two conjugate normal faults cutting the entire succession from Buntsandstein into the Pleistocene sediments. The eastern fault of this structure reveals growth (Fig. 12). It causes the BUT, BJ, BUC and BT

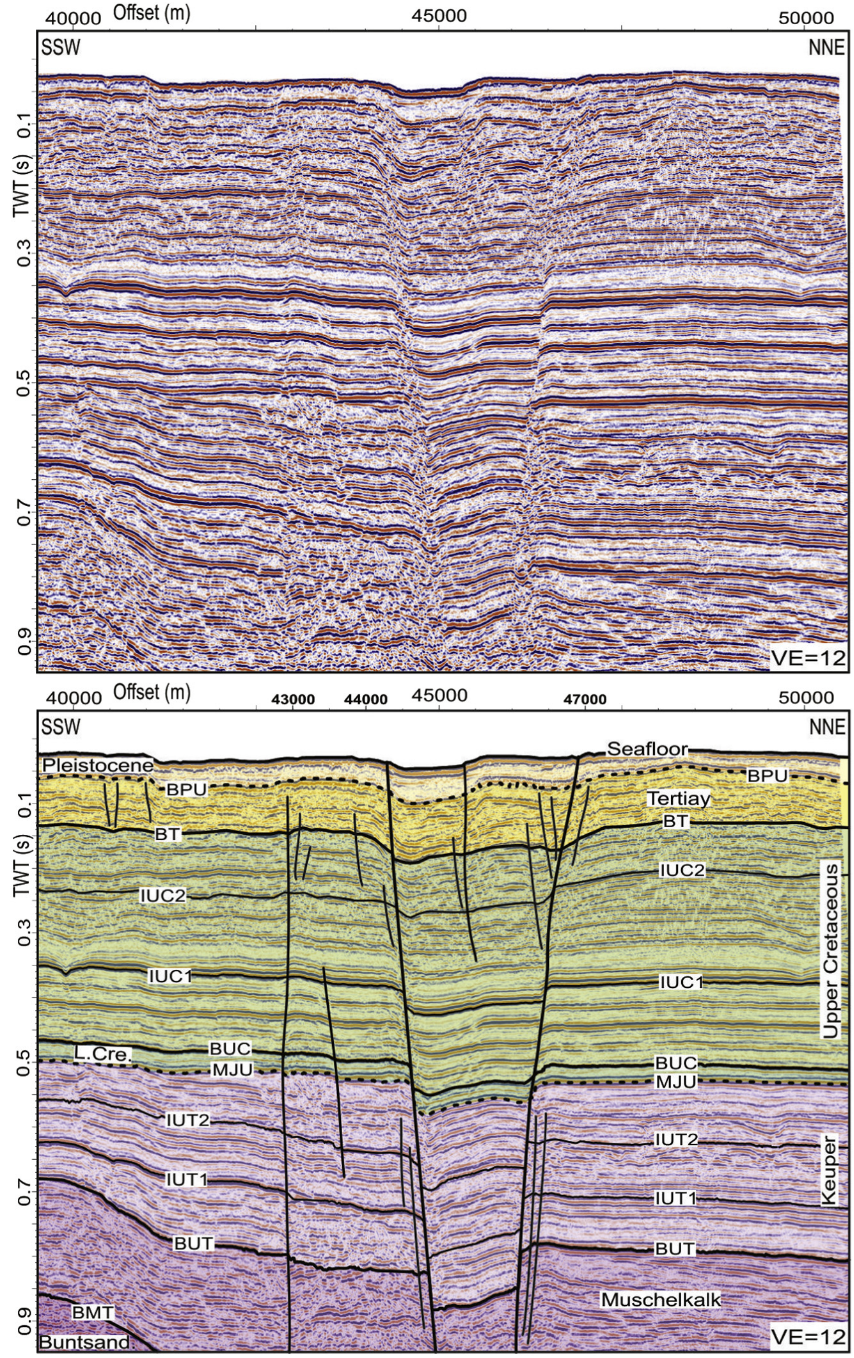

Fig. 10. SSW-NNE time-migrated seismic section (for location, see Fig. 2b) and interpreted section northeast of Langeland Island. Two conjugate faults cut the succession from Triassic into Pleistocene deposits. They reach upwards across the Pleistocene sediments, piercing the seafloor horizon. Black lines mark fault systems. BMT: Base Middle Triassic; BPU: Base Pleistocene Unconformity; BT: Base Tertiary; BUC: Base Upper Cretaceous; BUT: Base Upper Triassic; IUC 1 and 2: Internal Upper Cretaceous 1 and 2; IUT 1 and 2: Internal Upper Triassic 1 and 2; and MJU: Mid Jurassic Unconformity.

horizons to fall by ~270 m, 240 m, 180 m and 115 m, respectively. More faults are present further west.

The SW-NE seismic section in Fig. 13 is located north of the Grimmen High, crossing the Werre and Prerow fault systems (Fig. 2b). Between offsets 14,000 m and 17,500 m, two major conjugate faults cut the entire succession from Triassic into Pleistocene sediments, forming a graben structure (Fig. 13). These faults correspond to the Werre and Prerow fault systems (Krauss and Mayer, 2004). Both faults propagate upwards and cut the BPU horizon.

The seismic profile in Fig. 14 strikes SW-NE, crossing the Agricola Fault system described by Krauss and Mayer (2004) (Fig. 2b). It shows several normal faults are cutting the strata from the Jurassic-Triassic rocks into the Pleistocene deposits. At offset 38,000 m, one of these faults reaches upwards, penetrating the seafloor (Fig. 14). Some other faults intersect the succession from Jurassic-Triassic into the Upper Cretaceous sediments. The Agricola Fault system is mostly concentrated on the pinch out of the salt (Fig. 18).

The Skurup, Romeleasen and Vomb Faults are imaged in Fig. 15. At offset 82,500 m, one reverse fault represents the northern prolongation of the Vomb Fault as described by Schlüter et al. (1998). The fault cuts the entire succession from Jurassic-Triassic rocks across the Upper Cretaceous unit and penetrants the BPU horizon. The BUC horizon shows a vertical displacement of ~625 m, accordingly. Further to the west, the

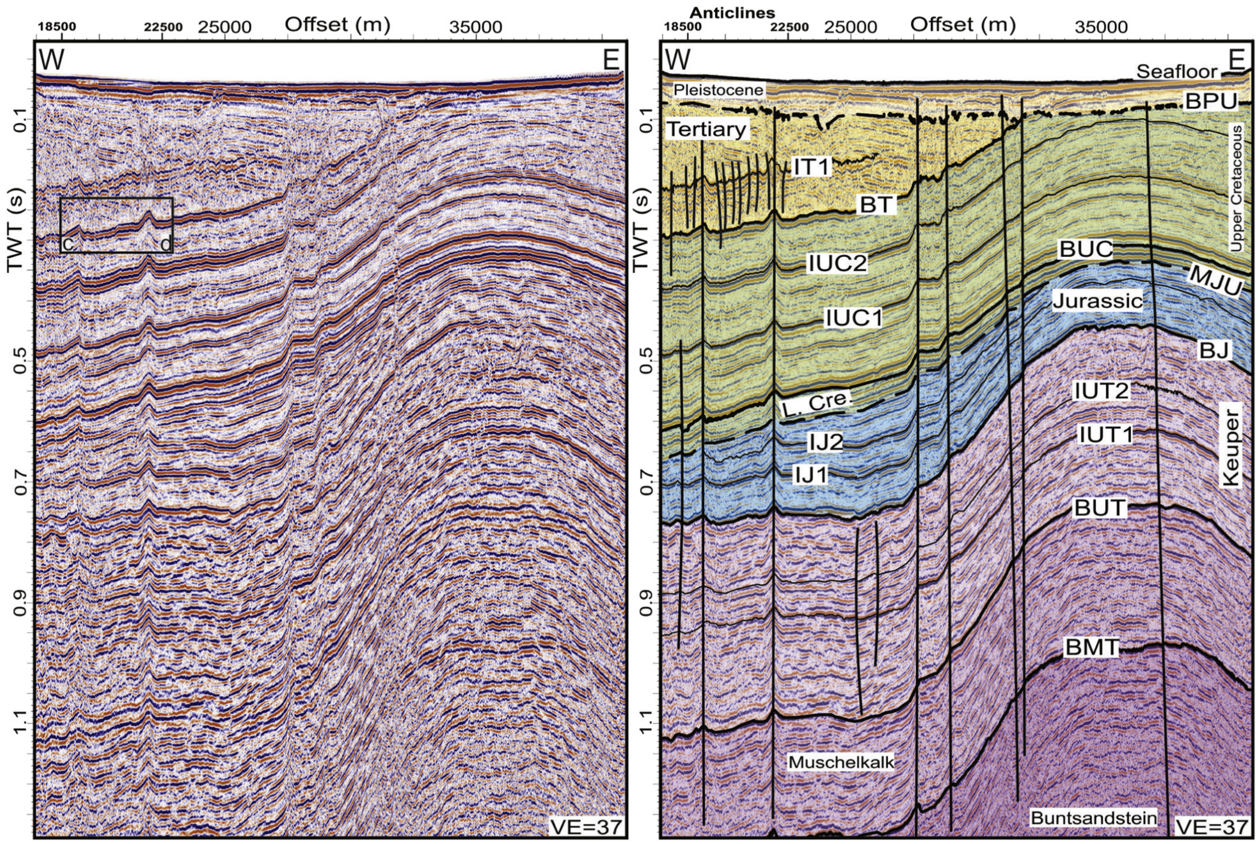

Fig. 11. W-E time-migrated seismic section(for location, see Fig. 2b) and interpreted section from the northwestern margin of the North German Basin. The eastern part of the section crosses the NW-SE salt pillow. Two V-shape anticlines are observed in the western part of the section. In the central of each anticline, a normal fault cuts through the entire succession from Muschelkalk into the Tertiary sediments. The eastern fault reaches upwards and cuts the BPU horizon. Several other faults cut through the entire succession and mostly intersect the Pleistocene sediments. BJ: Base Jurassic; BMT: Base Middle Triassic; BPU: Base Pleistocene Unconformity; BT: Base Tertiary; BUC: Base Upper Cretaceous; BUT: Base Upper Triassic; IJ 1 and 2: Internal Jurassic 1 and 2; IUC 1 and 2: Internal Upper Cretaceous 1 and 2; IUT 1 and 2: Internal Upper Triassic 1 and 2; and MJU: Mid Jurassic Unconformity.

Romeleasen Fault (Schlüter et al., 1998) cuts the succession from Jurassic-Triassic rocks into the Lower Maastrichtian deposits. At offset 42,500 m, the Skurup normal fault cuts the entire succession from the Paleozoic unit across the Upper Cretaceous layer and pierces the BUP horizon.

The seismic section in Fig. 16 crosses both the Adler-Kamien and Wiek Faults (Fig. 2b; Schlüter et al., 1998). The Wiek normal fault cuts the succession from Jurassic-Triassic rocks into the Pleistocene deposits. The eastern faults represent the Adler-Kamien thrust fault system that cuts the entire succession from Jurassic-Triassic rocks across the Upper Cretaceous and penetrants the BPU horizon. The Adler-Kamien Fault penetrates the BPU horizon only in this particular seismic line (Fig. 16).

At offset 14,500 m, the Wiek normal fault cuts the entire succession at least from the MJU horizon across the Upper Cretaceous into the Pleistocene deposits (Fig. 16). Blind faults are abundant within the Upper Cretaceous strata in both Figs. 15 and 16.

The seismic line in Fig. 17 runs SW-NE and is located above the NW-SE trending Øresund Fault. It also crosses the Carlsberg Fault with its eastern part (Fig. 2b). The Carlsberg Fault cuts the entire succession from Triassic rocks up to the seafloor (Fig. 17). Here, the seafloor horizon reveals depression. East of it, another normal fault cuts the strata at least from the Santonian into the Pleistocene deposits. This fault propagates upwards, penetrating the seafloor. Two normal faults are cutting the strata from Triassic into Cretaceous. Between offsets 5000 m and 15,000 m, several other faults intersect the Upper Cretaceous succession and are more abundant within the Maastrichtian sediments. For example, at offset 15,000 m, one of these faults reaches upwards across the Pleistocene deposits and pierces the seafloor.

5.2. Anticlines, near-vertical faults and tunnel valleys

Mesozoic and Tertiary deposits reveal anticlines, which are quite similar to those described by Al Hseinat and Hübscher (2014). The anticlines are more abundant in the northern Bays of Kiel and Mecklenburg, which is near the northwestern margin of the North German Basin (Fig. 23).

The shape of the observed anticlines varies from triangular (e.g., Figs. 8 and 9) to concentric (e.g., Fig. 11). They have a width of ~700 m to 3000 m. In most cases, their height decreases slightly with depth (e.g., Fig. 9). Assuming an average interval velocity of 2000 m/s to 3000 m/s (Hansen et al., 2007), the height of the anticlines ranges between ~ 20 m and 75 m. Their length ranges between ~2 km to 50 km (Fig. 23).

Some of the anticlines are associated with an erosional valley above (e.g., Figs. 8 and 9). As observed by Al Hseinat and Hübscher (2014) there is no relationship between the width of the anticline and the valley. In the salt influenced North German Basin, several anticlines are also associated with normal faults (Figs. 8, 9 and 23). It is notable that none of these anticlines is located above known salt pillow.

5.3. Major trends

Fig. 24 shows the basement faults compiled from previous studies (Baldschuhn et al., 1991, 1996, 2001; Bayer et al., 1999; Clausen and Pedersen, 1999; Krauss, 1994; Kossow et al., 2000; Lokhorst et al., 1998; Maystrenko et al., 2005a; NIA, 2000; Schlüter et al., 1997; Thomas et al., 1993; Vejbæk, 1997) and shallow faults based on this study. Basement faults in the study area are trending NW-SE, N-S

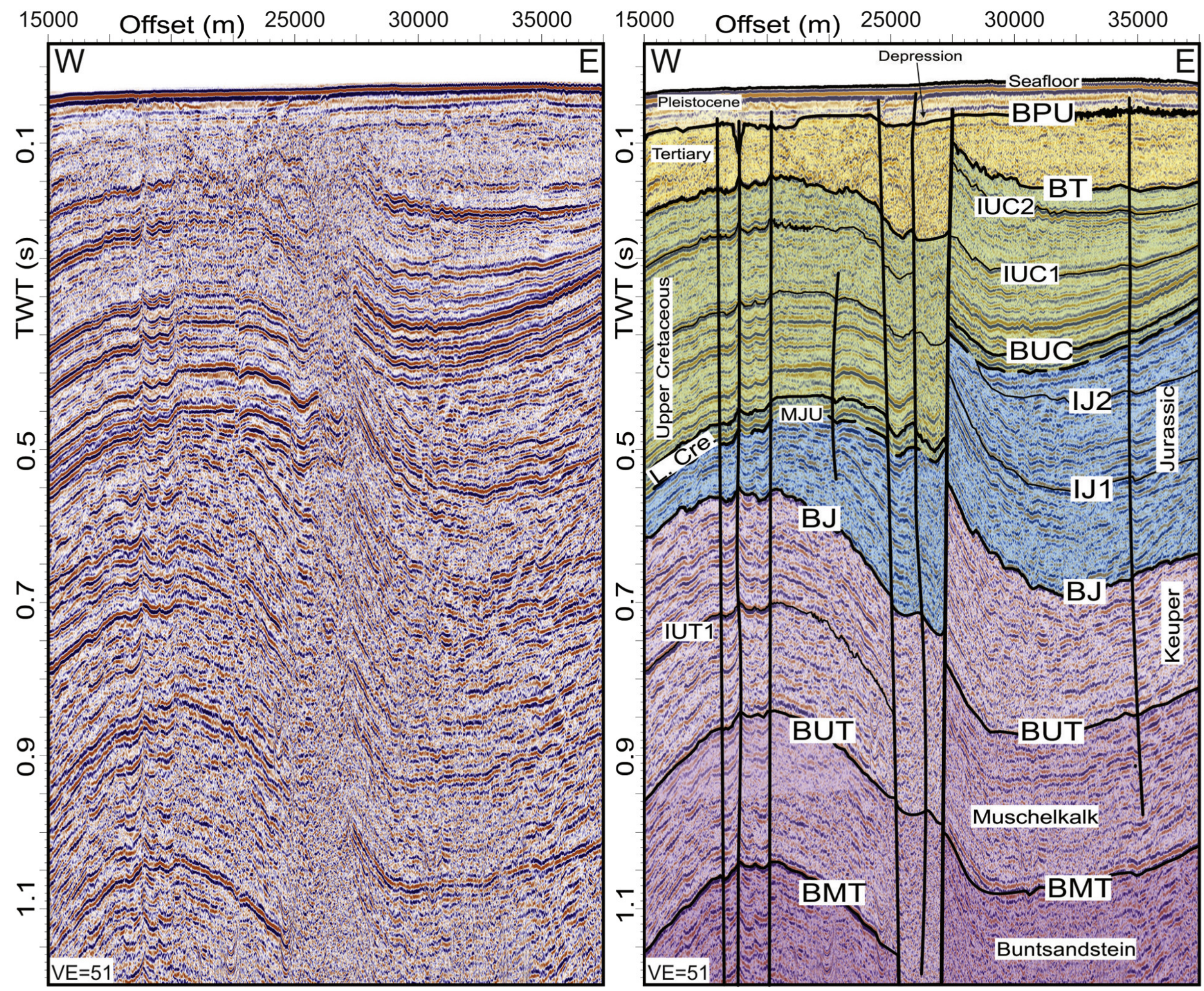

Fig. 12. W-E time-migrated seismic section (for location, see Fig. 2b) and interpreted section from the northern margin of the North German Basin. In the middle of the section, two conjugate normal faults cut the entire succession from Buntsandstein into the Pleistocene sediments. The eastern fault reveals growth. Other normal faults cut the entire succession into the Pleistocene sediments. BJ: Base Jurassic; BMT: Base Middle Triassic; BPU: Base Pleistocene Unconformity; BT: Base Tertiary; BUC: Base Upper Cretaceous; BUT: Base Upper Triassic; IJ 1 and 2: Internal Jurassic 1 and 2; IUC 1 and 2: Internal Upper Cretaceous 1 and 2; IUT 1 and 2: Internal Upper Triassic 1 and 2; and MJU: Mid Jurassic Unconformity.

(NNE-SSW) and minor NE-SW. The main structural elements are NW-SE directed: the Tornquist Zone, Caledonian Deformation Front, Adler-Kamien Fault and Elbe Lineament (Fig. 1). Minor NW-SE striking faults are the Langeland, Prerow and Werre Faults (Fig. 1). Several other major faults are trending N-S and parallel the Glückstadt Graben faults. Two major faults, the Agricola and Svedala Faults, have a NE-SW trending.

The salt influenced North German Basin reveals three major fault directions (Figs. 18–20): NW-SE, N-S and NNE-SSW, following the dominant direction of the major faults in the region. Several of these faults are located directly above basement (sub-salt) faults and salt pillows. The majority of these faults in the Bays of Kiel and Mecklenburg are trending N-S to NNE-SSW and parallel the direction of the Glückstadt Graben faults. Minor E-W faults are mapped in the Bay of Kiel above the almost E-W trending salt pillow. Similar faults were previously described by Hansen et al. (2005). Along the Store Belt, a group of E-W striking faults observed for the first time. Comparison with Fig. 1 reveals that this group of fault traces parallels the trend of the Caledonian Deformation Front.

The salt free Tornquist Zone (Pomeranian Bay) reveals two major fault trends of the Cretaceous and Pleistocene faults (Figs. 18 and 20): NW-SE and NE-SW. The majority of these faults are located above basement faults following the trend of the Tornquist Zone (Fig. 18). Also, the N-S to NNE-SSW directed Pleistocene tunnel valleys parallel the dominant trend of major faults e.g., “b” and “c” in Fig. 20. Other trends of the Pleistocene tunnel valleys are observed: (i) an E-W trending tunnel valleys in the Mecklenburg Bay and Arkona Basin marked “e” and “g” in Fig. 20; and (ii) a NE-SW striking tunnel valley northeast of Darß Island.

As mentioned in the previous section, anticline structures are only observed within the salt influenced North German Basin, particularly within the Bays of Kiel and Mecklenburg (Fig. 23). The main anticlines, such as a and b in Fig. 23, run N-S to NNE-SSW and show apparent coincidence with the N-S direct fault pattern of the Glückstadt Graben.

6. Interpretation and discussion

The Upper Cretaceous and Tertiary layers reveal numerous faults throughout the southwest Baltic Sea (Figs. 18–19). Several of these faults cross the entire sedimentary succession from Triassic up to the Pleistocene (Figs. 5–17). The spatial density of those faults is more abundant in the salt influenced North German Basin than in the salt free Tornquist Zone (Pomeranian Bay).

Previous studies of the southern Baltic have focused on the Mesozoic structural evolution (Hansen et al., 2005, 2007; Hübscher et al., 2010; Krauss and Mayer, 2004; Schlüter et al., 1997, 1998). Consequently, we will discuss these events briefly and will focus on the discussion of the Late Cretaceous to recent structural evolution.

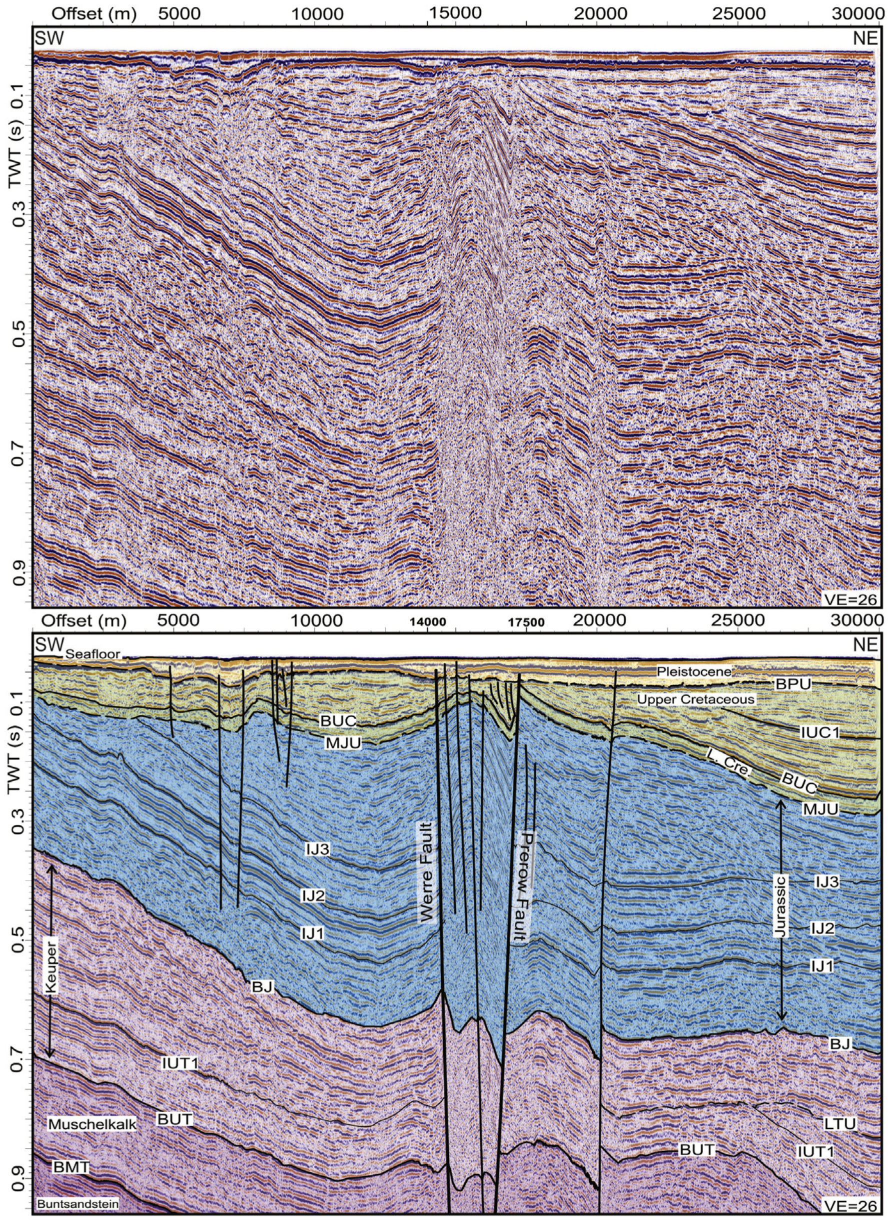

Fig. 13. SW-NE time-migrated seismic section (for location, see Fig. 2b) and interpreted seismic section crosses the Werre and Prerow Faults. These faults are conjugate faults cut the entire succession from Triassic into Pleistocene sediments, causing a graben structure. Both faults reach upwards, cutting the BPU horizon. Several faults intersect the PBU horizon. BJ: Base Jurassic; BMT: Base Middle Triassic; BPU: Base Pleistocene Unconformity; BT: Base Tertiary; BUC: Base Upper Cretaceous; BUT: Base Upper Triassic; IJ 1, 2 and 3: Internal Jurassic 1, 2 and 3; IUC 1: Internal Upper Cretaceous 1; IUT 1: Internal Upper Triassic 1; LTU: Late Triassic Unconformity; and MJU: Mid Jurassic Unconformity.

6.1. Triassic extension and Jurassic uplift

During the early Late Triassic and Early Jurassic, a regional E–W directed extensional tectonic regime affected the North German Basin and adjacent areas (Fig. 3; Ziegler, 1990) and created the deep-rooted basement faults. The extension is indicated near the Glückstadt Graben by accelerated subsidence and basement-affected normal faulting (e.g., Fisher and Kockel, 1999; Fisher and Mudge, 1998; Scheck et al., 2003b; Ziegler, 1990) within the salt influenced basin (Fig. 2b). Salt diapirism initiation within the Bays of Kiel and Mecklenburg was interpreted as a result of this extensional event (Al Hseinat and Hübscher, 2014; Al Hseinat et al., 2016; Hansen et al., 2005, 2007; Hübscher et al., 2010). Accordingly, we interpret salt diapirism initiation in Figs. 7 and 8 and vertical salt movement with a pillow-like structure due to the ongoing regional extension during the early Late Triassic and Early Jurassic.

Later on, the development of the central North Sea Dome (Middle Jurassic to Early Cretaceous), due to a mantle plume (Underhill, 1998; Ziegler, 1990), caused a period of uplift and non-deposition. Consequently, parts of the Jurassic and Upper Triassic sedimentary successions in the region were eroded (Al Hseinat and Hübscher, 2014; Hansen et al., 2005; Hübscher et al., 2010; Kossow et al., 2000). In this study, this event is marked by a clear angular unconformity (MJU) evident in all seismic sections (Figs. 5–17). The subsequent Early Cretaceous period was a time of tectonic quiescence and rising sea levels (Kossow and Krawczyk, 2002).

6.2. Late Cretaceous-Early Paleogene inversion

A prominent change in the regional stress field, from extension to compression, took place at the Late Cretaceous-Early Paleogene transition (Ziegler, 1990). It resulted from two phases: major plate reorganisation

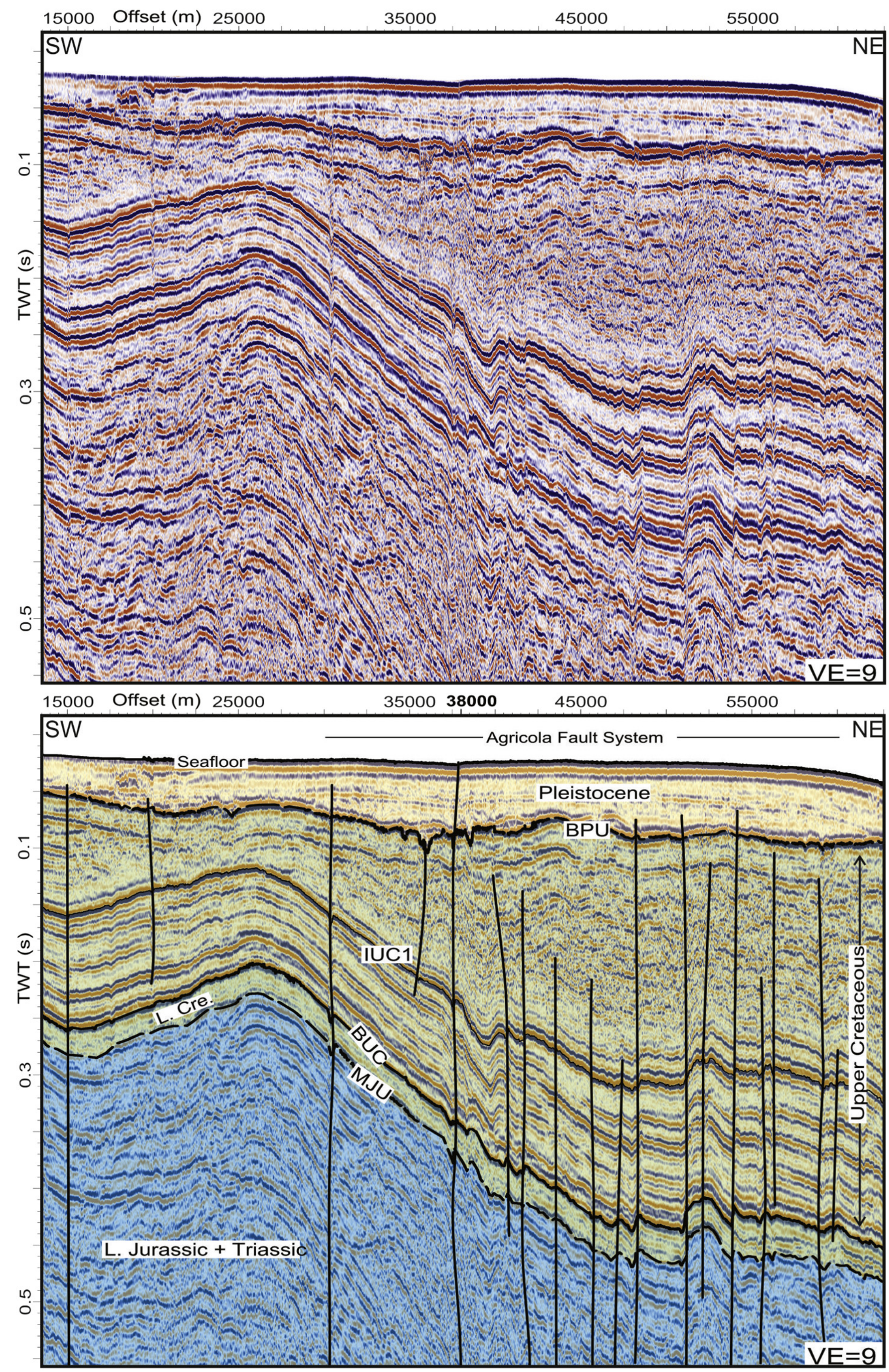

Fig. 14. SW-NE time-migrated seismic section (for location, see Fig. 2b) and interpreted seismic section crosses the Agricola Fault system. Several normal faults are observed. Most of them intersect the strata from the Jurassic-Triassic rocks into the Pleistocene deposits. One fault even propagates upwards, piercing the seafloor horizon. BPU: Base Pleistocene Unconformity; BUC: Base Upper Cretaceous; IUC 1:Internal Upper Cretaceous 1; and MJU: Mid Jurassic Unconformity.

related to the Africa-Iberia-Europe convergence and the subsequent Alpine Orogeny (~90 Ma) (Bayer et al., 1999; Kley and Voigt, 2008; Krauss, 1994; Scheck-Wenderoth and Lamarche, 2005; Ziegler, 1990). The compression affected all of Europe. Reactivation of pre-existing fault systems, vertical salt movements and inversion of former basins or troughs are believed to be the result of the combination of the previously mentioned plate motions (Kockel, 2003; Kley and Voigt, 2008). Clausen and Huuse (1999) described a Late Cretaceous-Paleogene inversion of the basement structures south of the Ringkøbing-Fyn High that deformed most of the Upper Cretaceous and Tertiary successions in a compression event. According to Hansen et al. (2005), the NE-SW to NNE-SSW directed compressive stress field (Late Cretaceous-Early Tertiary) confirms that the N-S striking supra-salt fault above the salt pillow within the Bay of Kiel developed thin-skinned as a result of halokinesis. We interpret the tectonic evolution of the supra-salt faults within the salt influenced North German Basin accordingly (Figs. 7 and 8).

The calculated Base Upper Cretaceous time-structure map (Fig. 18) shows that the area between Darß and Falster Islands

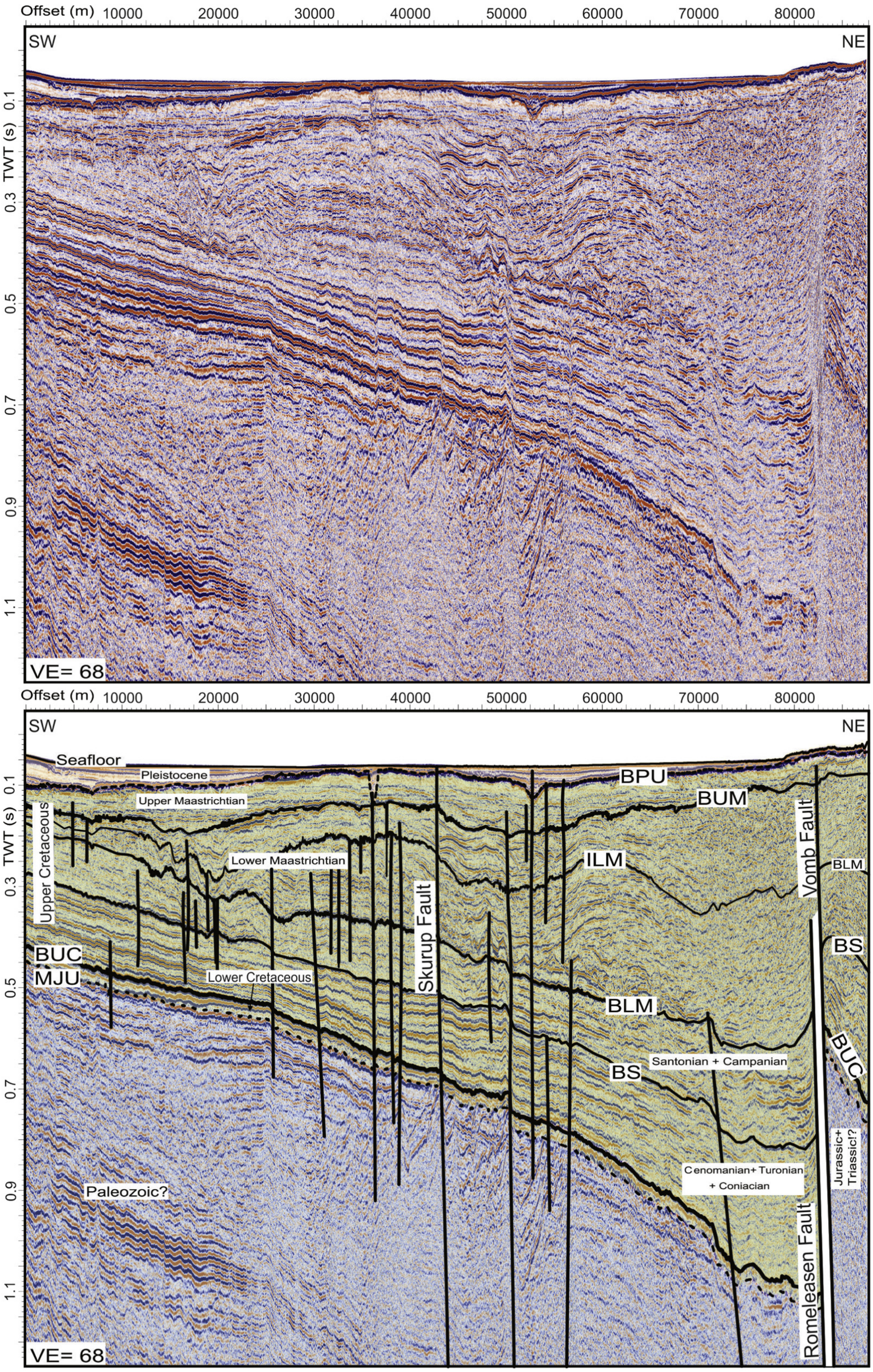

Fig. 15. SW-NE time-migrated seismic section (for location, see Fig. 2b) and interpreted seismic section crosses the transition from Arkona block to Skurup Block. This section also shows the Skurup Fault, Romeleasen Fault and Vomb Faults. The Skurup and Vomb Faults cut the Upper Cretaceous succession and reach upwards piercing the BPU horizon. Several faults intersect the Upper Cretaceous succession and at least two of them propagate, penetrating the BPU. BLM: Base Lower Maastrichtian; BPU: Base Pleistocene Unconformity; BS: Base Santonian; BUC: Base Upper Cretaceous; BUM: Base Upper Maastrichtian ILM: Internal Lower Maastrichtian; and MJU: Mid Jurassic Unconformity.

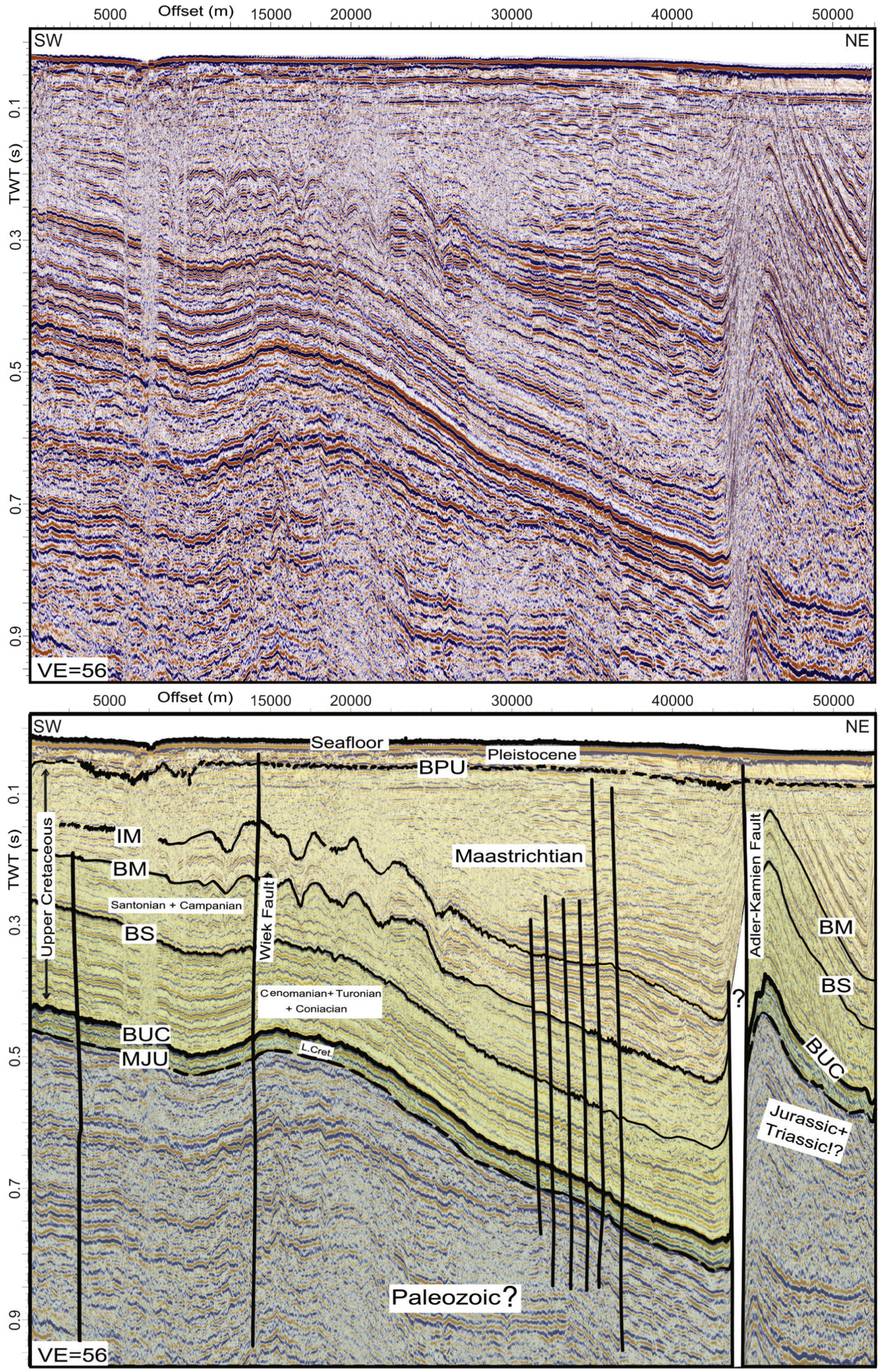

Fig. 16. SW-NE time-migrated seismic section (for location, see Fig. 2b) and interpreted seismic section crosses the Gryfice Graben. It also shows the Wiek Fault and two faults of the Adler-Kamien Fault System. BM: Base Maastrichtian; BPU: Base Pleistocene Unconformity; BS: Base Santonian; BUC: Base Upper Cretaceous; BUM: Base Upper Maastrichtian IM: Internal Maastrichtian; and MJU: Mid Jurassic Unconformity.

(Kadett Channel) reveals uplift, which is consistent with the observations made by others (Hübscher et al., 2010; Kossow and Krawczyk, 2002).

However, in contrast to other basins of the CEBS, the Glückstadt Graben was essentially not inverted (Grassmann et al., 2005; Maystrenko et al., 2005a). We speculate that the absent inversion is a consequence of

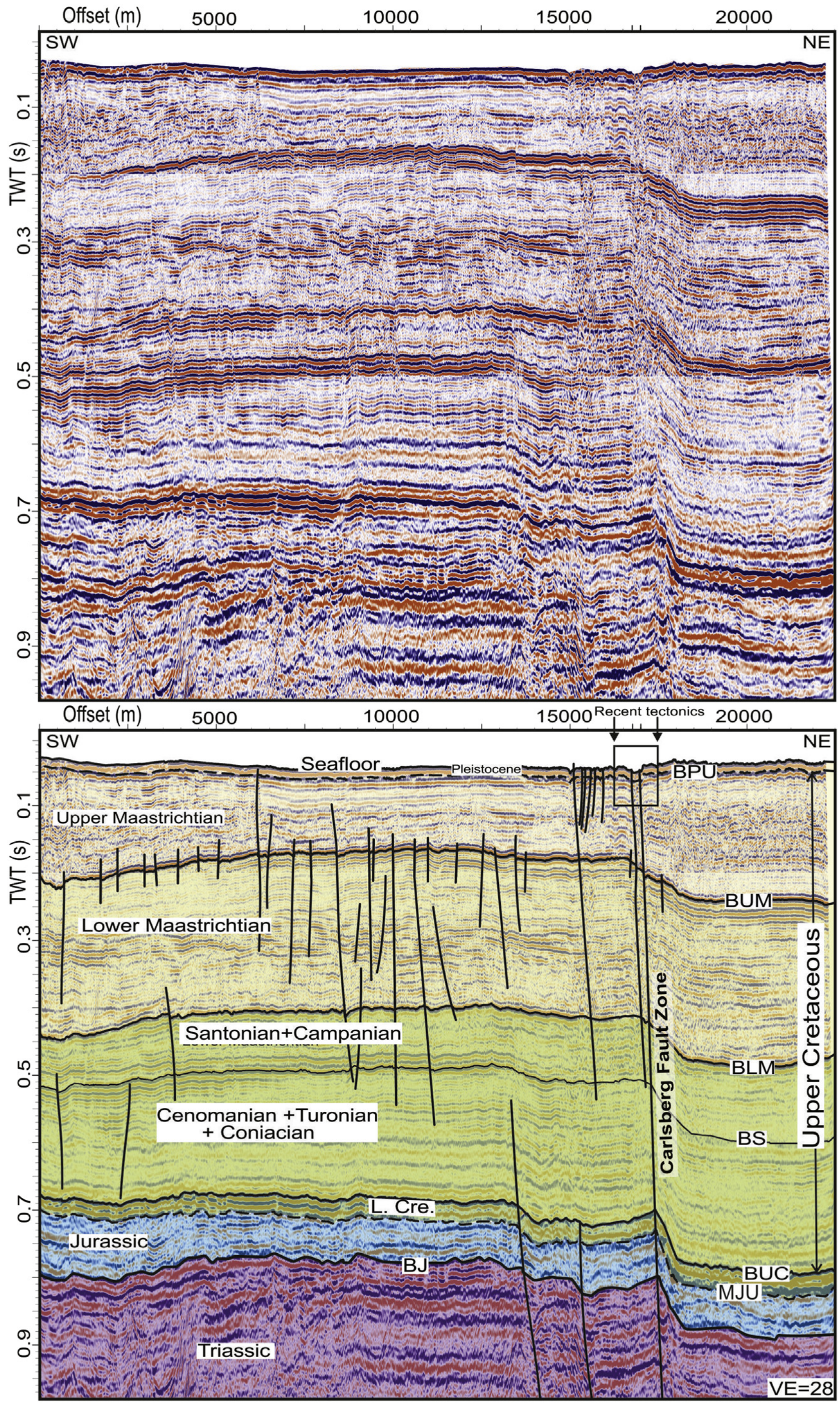

Fig. 17. SW-NE time-migrated seismic section (for location, see Fig. 2b) and interpreted seismic section crossing the Øresund Fault. It is also crosses the Carlsberg Fault. Carlsberg Fault cuts the entire suction from Triassic into the Pleistocene deposits. It is also piercing the seafloor horizon. BJ: Base Jurassic; BLM: Base Lower Maastrichtian; BPU: Base Pleistocene Unconformity; BS: Base Santonian; BUC: Base Upper Cretaceous; BUM: Base Upper Maastrichtian; and MJU: Mid Jurassic Unconformity.

the almost rectangular angle between the Glückstadt Graben and the intraplate contraction between Africa and Europe. Considering the contraction as $\sigma1$, one would expect extension in $\sigma3$ direction, which would result in the extension of the Glückstadt Graben rather than an inversion.

Recent studies within the southwest Baltic Sea related Cretaceous evolution of some faults, initiation of vertical salt movement and supra-salt faulting to the Late Cretaceous-Early Tertiary inversion-induced reactivation of a deep-rooted fault (e.g., Al Hseinat and Hübscher, 2014; Al Hseinat et al., 2016; Kammann et al., 2016).

Significant displacement of the Upper Cretaceous sediments (Figs. 12 and 16) can be related to the same inversion event. This is in good agreement with the observations made by others (e.g., Hübscher et al., 2010; Schlüter et al., 1997, 1998). Similar observations were made by Brandes et al. (2012a, 2013) in the Subhercynian Basin at the southern margin of the CEBS.

We therefore explain the Late Cretaceous reactivation of older fault systems within the study area and initiation of the supra-salt faults by the Late Cretaceous-Early Tertiary compressional events.

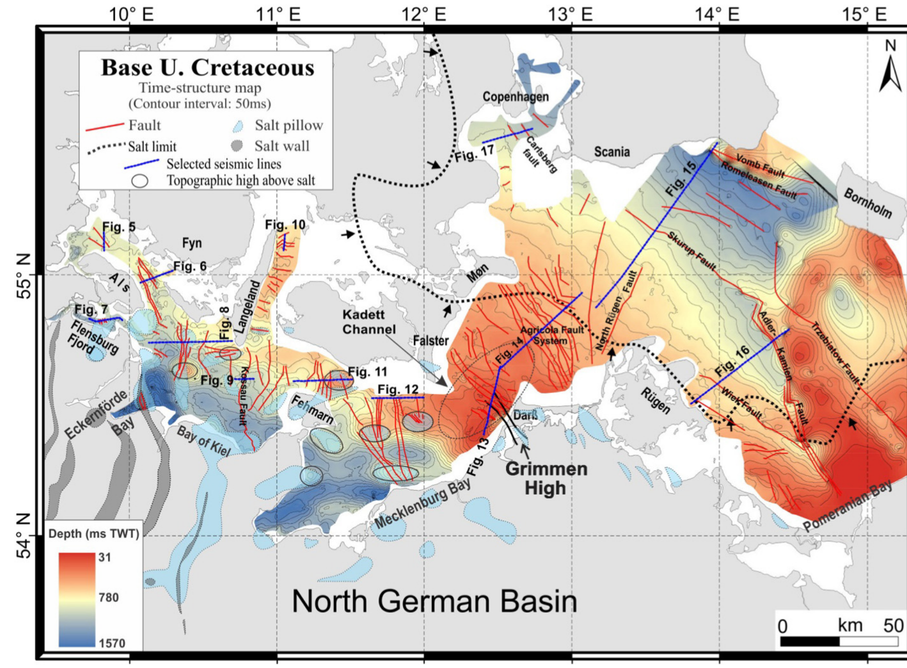

Fig. 18. Time-structure map of the Base Upper Cretaceous surface in ms TWT. Contour interval is 50 ms. The distribution of salt walls and pillows are from Lokhorst et al. (1998). The red-orange colors show the shallowest parts of the surface, whereas the blue color shows the deepest parts. (For interpretation of the references to color in this figure legend, the reader is referred to the web version of this article.)

6.3. Upper Tertiary extension

Several Cretaceous and Tertiary faults show upward extension into the unconsolidated Pleistocene sediments (Figs. 11–16 and 19). The upward extension of these faults most likely reflects the Neogene to recent NW–SE directed extension of the CEBS. This observation is in good agreement with Grassmann et al. (2005) and Kley et al. (2008) interpretations.

The absence of Tertiary deposits above a salt diapir that rests on an N-S trending fault related to the Glückstadt Graben documents a halokinetic phase during Tertiary in the central Bay of Kiel (Hansen et al., 2005). Grassmann et al. (2005) and Maystrenko et al. (2005a) discussed the evolution of the eastern margin of the Eastholstein Trough by means of reflection seismic data. They observed a vertical displacement of the BT horizon of ~1 s TWT, which corresponds to >1000 m assuming an average interval velocity of the Tertiary of >2 km/s. Furthermore, Al Hseinat and Hübscher (2014) and Al Hseinat et al. (2016) attributed Tertiary to recent halokinetics and faulting in the supra-Zechstein succession in the

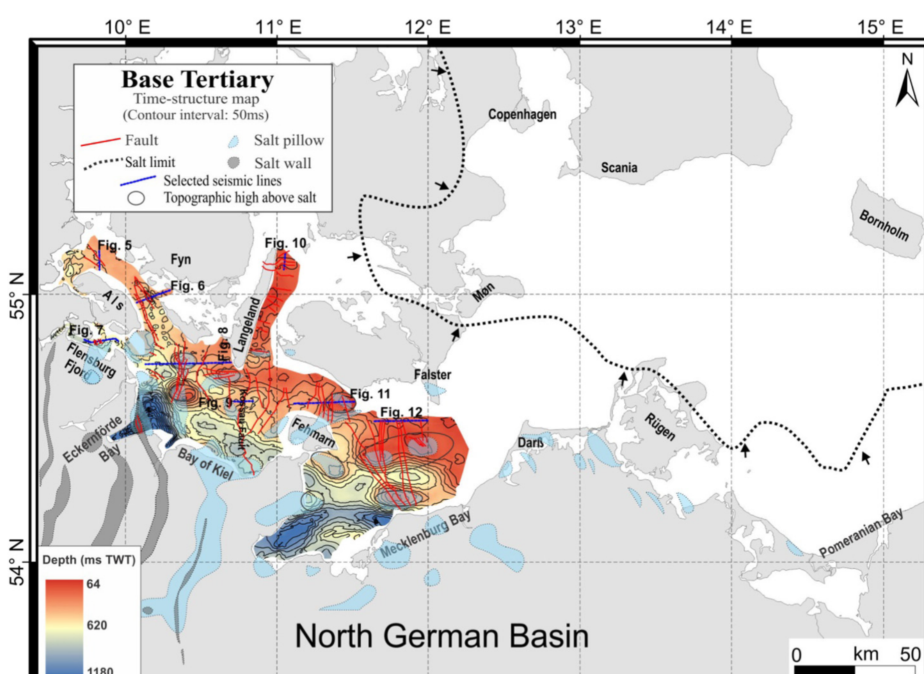

Fig. 19. Time-structure map of the Base Tertiary surface in ms TWT. Contour interval is 50 ms. The distribution of salt walls and pillows are from Lokhorst et al. (1998). The red-orange colors show the shallowest parts of the surface, whereas the blue color shows the deepest parts. (For interpretation of the references to color in this figure legend, the reader is referred to the web version of this article.)

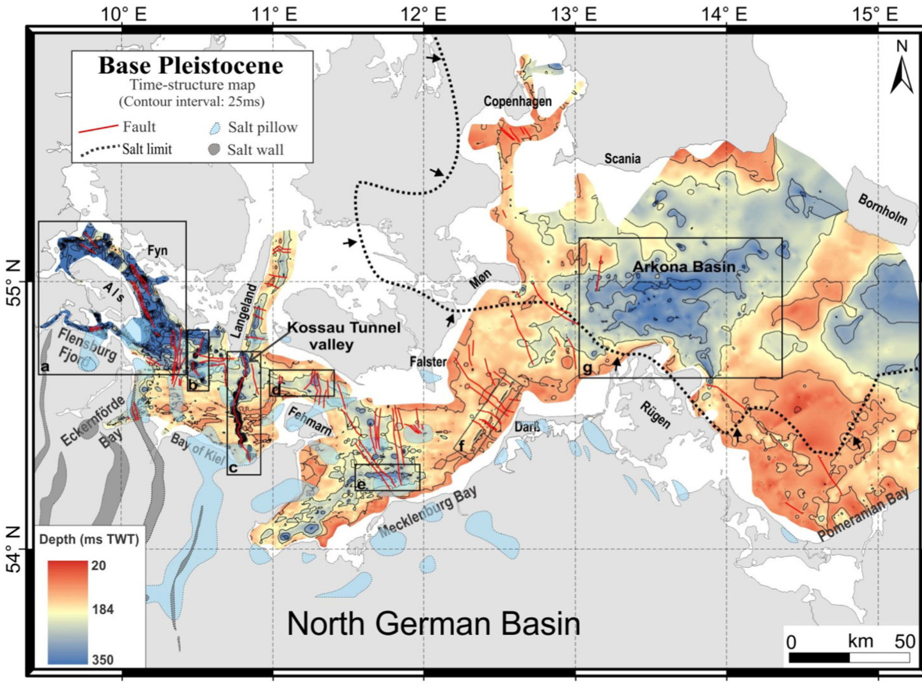

Fig. 20. Time-structure map of the Base Pleistocene surface in ms TWT. Contour interval is 25 ms. The distribution of salt walls and pillows are from Lokhorst et al. (1998). Black rectangles (a–g) mark major topographic lows. The red-orange colors show the shallowest parts of the surface, whereas the blue color shows the deepest parts. (For interpretation of the references to color in this figure legend, the reader is referred to the web version of this article.)

southwest Baltic Sea to the Neogene to recent NW-SE directed extension of the Glückstadt Graben.

6.4. Pleistocene until Upper Holocene tectonics

Varied stratigraphic observations strongly suggest that fault evolution continued during the Pleistocene until today (Figs. 5–17). It is notable that the density of subsurface (shallow) faults is much higher in the salt influenced North German Basin compared to the salt free Tornquist Zone (Pomeranian Bay) (Fig. 19).

This finding raises the question as to what is actual the cause of recent tectonics. There are two possible candidates: Ice-load induced tectonics and present-day stress field.

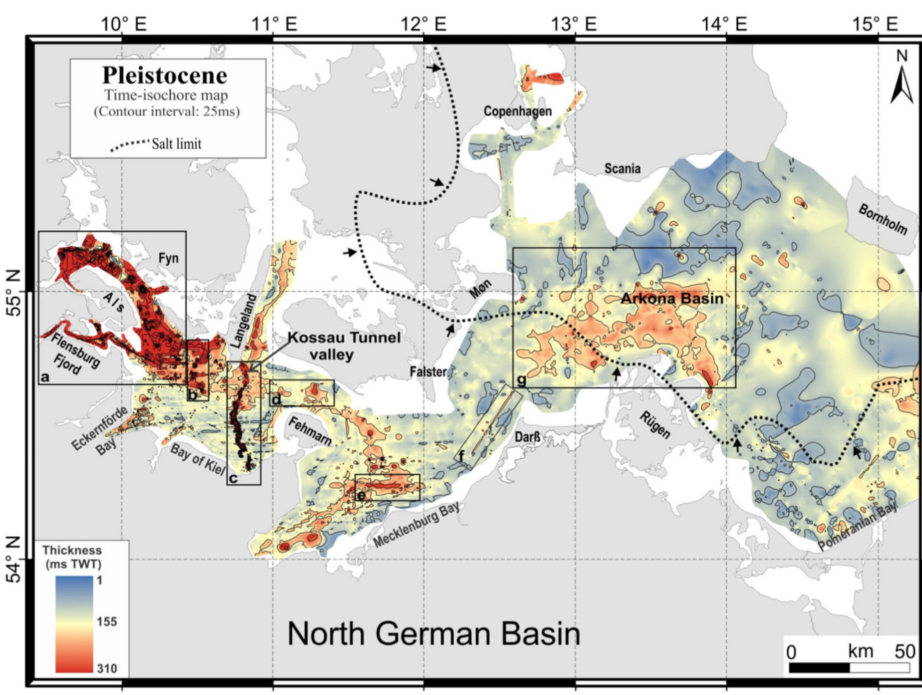

Fig. 21. Time-isochore map of the Pleistocene succession (time-interval map) in ms TWT. Black rectangles (a–g) mark major and minor thickness anomalies. Contour interval is 25 ms. There d-orange colors show the thickest parts, while the yellow-blue colors show the thinnest parts. (For interpretation of the references to color in this figure legend, the reader is referred to the web version of this article.)

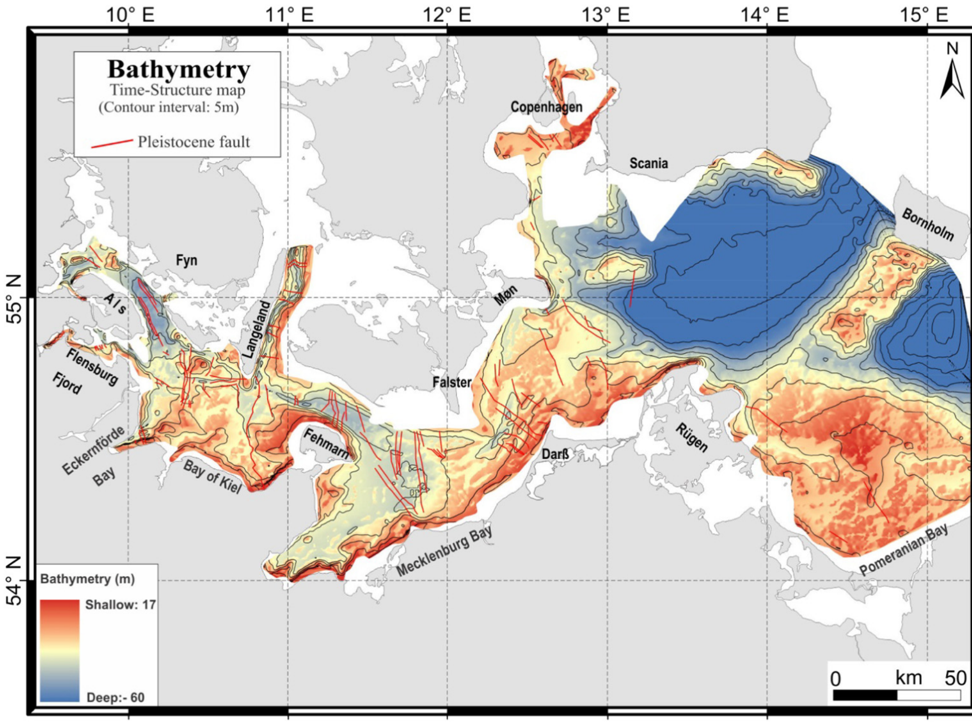

Fig. 22. Bathymetry of the study area (based on Seifert et al., 2001). Pleistocene faults are based on this study. Contour interval is 5 m. The blue color shows the deepest parts, while the red color shows the shallowest parts. (For interpretation of the references to color in this figure legend, the reader is referred to the web version of this article.)

6.4.1. Ice-loading/unloading induced tectonics

The prevailing regional tectonic stress in North Europe is caused by the ongoing Alpine collision and the spreading in the Central Atlantic, overprinted by glacial stresses (Roth and Fleckenstein, 2001). The ice movement direction was approximately NE-SW to NNE-SSW and perpendicular to the present shoreline of the Baltic Basin (Fig. 4; Piotrowski, 1997; Piotrowski and Tulaczyk, 1999). Repeated ice sheet loading and unloading during the Pleistocene caused vertical and horizontal stress variation, which led to a change in the equilibrium situation of the lithosphere and mass movements in the upper and lower mantle (e.g., Al Hseinat and Hübscher, 2014; Arvidsson, 1996; Brandes et al., 2012a, 2012b; Dyke et al., 1991; Fenton, 1994; Johnston, 1987; Kujansuu, 1964; Lagerbäck, 1978; Lagerbäck and Sundh, 2008; Lang et al., 2014; Munier and Fenton, 2004; Muir-Wood, 2000; Olesen, 1988; Quinlan, 1984; Sandersen and Jørgensen, 2015; Sauber and Molnia, 2004; Shilts et al., 1992; Steffen et al., 2014a, 2014b, 2014c, 2016; Steffen and Wu, 2011; Stewart et al., 2000; Turpeinen et al., 2008; Wu et al., 1999).

As combined by GIA models, the rebound's influence of the last glacial advance is still happing and will continue for another few thousand years (e.g., Kumar and Sunil Singh, 2012; Le Meur, 1996; Steffen and Wu, 2011). According to Stewart et al. (2000), the glacio-isostatic recovery from the glaciations therefore potentially had an impact on large areas not only within limits former ice sheet but also hundreds of

Table 1
Characteristics (fault type, displacement, length, possible correlation with deep rooted fault system) of those shallow faults that propagate into Pleistocene deposits or up to seafloor (for locations, see Figs. 1 and 2b).

Fig. number	Location	Salt	Correlated basement fault system	Direction	Max. length (km)	Fault type	Affected units	Max. offset (m)
5	Lille Belt	Yes	TF/RFH	NW-SE	11	Normal	Tr-SF	5
6	Lille Belt	Yes	TF/RFH	NW-SE	30	Normal	Tr-SF	5
7	Flensburg Fjord	Yes	GG	NNW-SSE	2	Normal	Tr-SF	30
8	Bay of Kiel	Yes	EHB	NNE-SSW	25	Normal	Tr-SF	130
9	Bay of Kiel	Yes	EHMB	N-S	50	Reverse	Tr-SF	7
10	Store Belt	Yes	CDF	E-W	8	Normal	Tr-SF	50
11	Fehmarn Belt	Yes	TF/RFH	NW-SE	15	Normal	Tr-SF	60
12	Mecklenburg Bay	Yes	Langeland Fault	NW-SE	32	Normal	Tr-SF	270
13	Between Darß and Falster	Yes	Grimmen High (Perow and Werre Faults)	NW-SE	36	Crestal Collapse Graben (strike-slip?)	Tr-SF	80
14	Northwest of Rügen	No	AFS	NE-SW	70	Normal	Ju-Pl	36
15	Arkona Block	No	VF SKF RF	NW-SE	32	Reverse	Ju-Pl	625
						Normal	Pal-Pl	25
						Normal	Pal-UC	
16	East of Rügen	No	AK F	NW-SE	70	Reverse	Ju-UC	625
			WF		40	Normal	Ju-Pl	12
17	South of Copenhagen	No	ØF + CF	NNW-SSE	8	Normal	Tr-SF	120

AFS: Agricola Fault System; AKF: Adler-Kamien Fault; CDF: Caledonian Deformation Front; CF: Carlsberg Fault; EHT: Eastholstein Trough; EHMB: Eastholstein Mecklenburg Trough; GG: Glückstadt Graben; Ju: Jurassic; ØF: Øresund Fault; Pal: Paleozoic; Pl: Pleistocene; RFH: Ringkøbing-Fyn High; RF: Romeleasen Fault; SF: seafloor; TF: Tornquist Fan; Tr: Triassic; UC: Upper Cretaceous; VF: Vomb Fault; and WF: Wiek Fault.

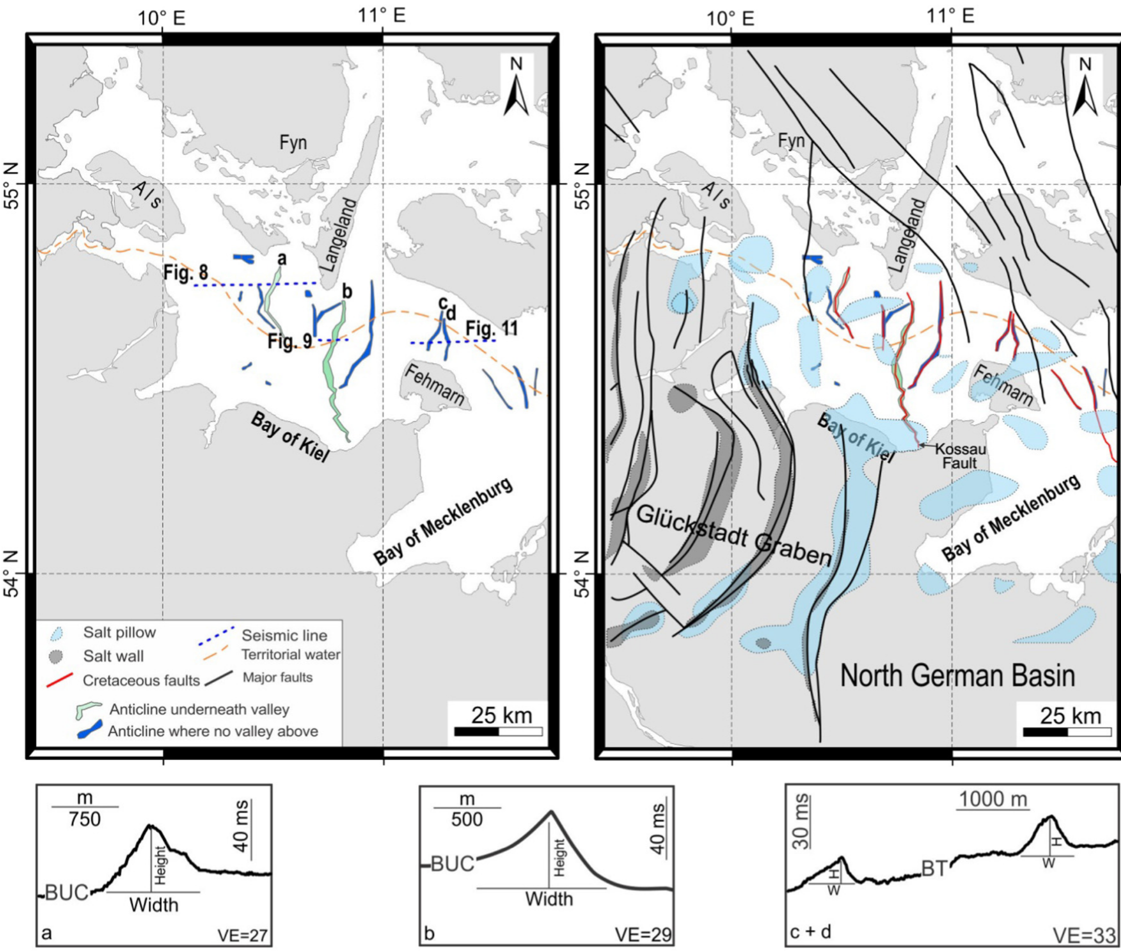

Fig. 23. Anticline structures in northwestern margin of the North German Basin. The approximate location of the major faults is compiled from Baldschuhn et al. (1991), Bayer et al. (1999), Clausen and Pedersen (1999), Krauss (1994), Kossow et al. (2000) and Maystrenko et al. (2005a). Cretaceous faults are from this study. The distribution of salt walls and pillows are from Lokhorst et al. (1998). The anticlines marked "a" and "b" are from Figs. 8 and 9, while "c" and "d" are from Fig.11. BUC: Base Upper Cretaceous; and BT: Base Tertiary.

kilometres beyond. They also pointed out how the ice sheet cycles may modulate not only the deep-seated viscoelastic response of the Earth, but also the nature and incidence of upper-crustal faulting, in addition to earthquake generation. Sirocko et al. (2008) introduced several conceptual models for the interaction between ice-loading/unloading and subsurface faults. One of these models describes how diapir rise is hindered and how faults are blocked during glaciation. After the ice sheets retreat, the salt rises once again and faults are reactivated. Recent outcomes of Al Hseinat and Hübscher (2014) and Lang et al. (2014) offer possible explanations for recent faulting by ice-load induced salt flow and fault reactivation without sub-salt tectonics. That effect on the salt wall stopped once ice grew over the whole structure, at which time the wall subsided because of ice loading. The salt wall and faults were reactivated again once the ice front retreated so that the ice loaded only one side of the structure.

Recent surface deformation of several millimetres per year along lineaments was observed in northern Germany (Lehné and Sirocko, 2010). Some of these lineaments coincide with the normal faults of the Glückstadt Graben and salt structures above (Fig. 2b). Lehné and Sirocko (2010) suggested that the deformation was most likely caused by an ongoing GIA since the Late Pleistocene Weichselian glacial maximum. By means of seismic data, Brandes et al. (2011) developed a tectonic model showing the reactivation of pre-existing faults within north-western Germany as a consequence of ice sheet loading/unloading.

Faults' reactivation due to GIA is more likely if the ice sheet advances normally in relation to the fault (Brandes et al., 2011; Stewart et al., 2000). According to these authors, faults that are orientated perpendicular to the orientation of the horizontal stress induced by ice sheet are believed to have a higher probability of being reactivated. Thus, the almost NW-SE, NNE-SSW and N-S striking faults within the southwest Baltic Sea are optimally orientated for ice-loading/unloading induced reactivation. This study suggests that this is valid for basically all faults trending more or less perpendicular to the elongated Baltic Basin. These observations are also in good agreement with Al Hseinat and Hübscher (2014) and Al Hseinat et al. (2016) who related the Pleistocene tectonics and subsurface (shallow) faulting in the southwest Baltic Sea to ice-load induced reactivation of older fault systems. In addition, the observed position of the Pleistocene faults directly above the Cretaceous and Tertiary faults confirms this assumption (Figs. 18–20).

Reicherter et al. (2005) and Stewart et al. (2000) calculated the approximate 3:1 ratio between ice thickness and lithospheric depression in the North German Basin (Fig. 25). As an example, according to this ratio, a 300 m thick ice layer generates a subsidence of 100 m. It is, therefore, a plausible assumption that even a relatively thin ice sheet of a few hundred metres thickness triggers subsurface faults. After ice retreats, the direction of the faults is inverted. Although this zero-order approximation oversimplifies the geological reality because it implies that the differential ice-load most likely reactivated pre-existing faults.

Faulting and folding beneath the ice sheet created a weakness zone that facilitated erosion by pressurized glacial and subglacial meltwater, which is the primary explanation for tunnel valley evolution (Al Hseinat and Hübscher, 2014; Huuse and Lykke-Andersen, 2000;

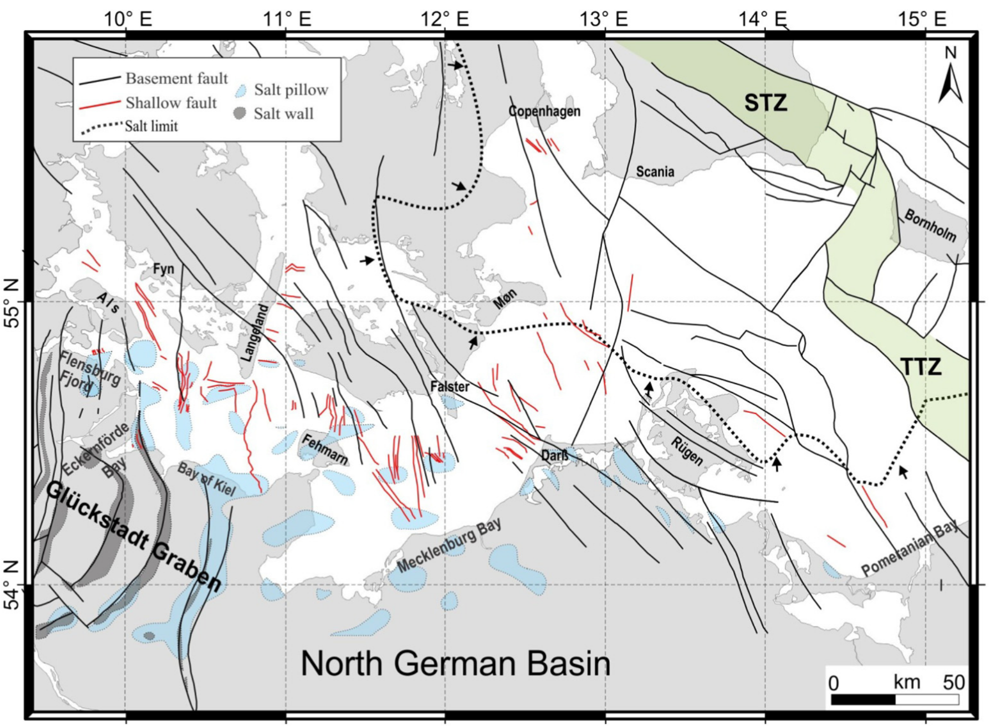

Fig. 24. Fault map of basement faults of the southwest Baltic Sea based on (Baldschuhn et al., 1991, 1996, 2001; Bayer et al., 1999; Clausen and Pedersen, 1999; Krauss, 1994; Kossow et al., 2000; Lokhorst et al., 1998; Maystrenko et al., 2005a; NIA, 2000; Schlüter et al., 1997; Thomas et al., 1993; Vejbæk, 1997) and shallow faults according to this study. STZ: Sorgenfrei-Tornquist Zone; and TTZ: Teisseyre-Tornquist Zone.

Jørgensen and Sandersen, 2004; Piotrowski, 1997). Recently, Al Hseinat and Hübscher (2014) related the formation and evolution of the Kossau Tunnel valley, marked "c" in Fig. 21, as a result of the interplay of ice-load induced tectonics and sub-glacial melt-water erosion. We may therefore conclude that the almost N-S directed tunnel valley, marked b in Fig. 21 was formed due to the same processes.

In contrast, the SW-NE orientated tunnel valley, marked "f" in Fig. 20, is previously interpreted as part of the drainage system at the beginning of the Baltic Ice Lake transgression (~11,500 years BP) (Lemke et al., 1994). It is described as the main water discharge system in the period immediately after retreating of the ice sheet. However, our available seismic information shows that the W-E and SW-NE directed tunnel valleys marked "e" and "f" in Fig. 20 are not connected.

The time-structure map of the Base Pleistocene shows that tunnel valleys are deeper if located directly above fault, e.g., "b" and "c" in Fig. 20. This is in agreement with the interpretations of Salomonsen (1993, 1995), who also observed a vertical correlation between Pleistocene tunnel valleys and faults beneath in the Danish North Sea Sector. Other authors have stated that the underlying structures may have had a local influence on the orientation of some valleys (e.g., Huuse and Lykke-Andersen, 2000; Lykke-Andersen et al., 1993; Sandersen and Jørgensen, 1998; Schwarz, 1996).

Normal faults associated with an anticline, as observed at the western margin of the North German Basin (Fig. 23), in the Triassic to Lower Tertiary strata could be interpreted as ice-load induced tectonics (e.g., Al Hseinat and Hübscher, 2014). These authors developed a conceptual model explaining the origins of a fault–anticline structure underneath the Kossau Tunnel valley within the Bay of Kiel as a consequence of ice-load induced tectonics above a pre-existing fault system.

6.4.2. Present-day stress field induced tectonics

Inherited fault planes of ancient tectonic deformations can be reactivated if they are either favorably or unfavorably oriented relative to the subsequent stress regimes (e.g., Bartholomew et al., 2002). Anyhow, the Pleistocene faults are more abundant within the salt influenced North German Basin than in the salt free Tornquist Zone (Fig. 19). One could speculate that the current NW-SE directed extension (Kley et al., 2008) should result in increased extension of all normal faults perpendicular to σ3. We assume that this is valid for essentially all faults trending more or less perpendicular to the elongated Baltic

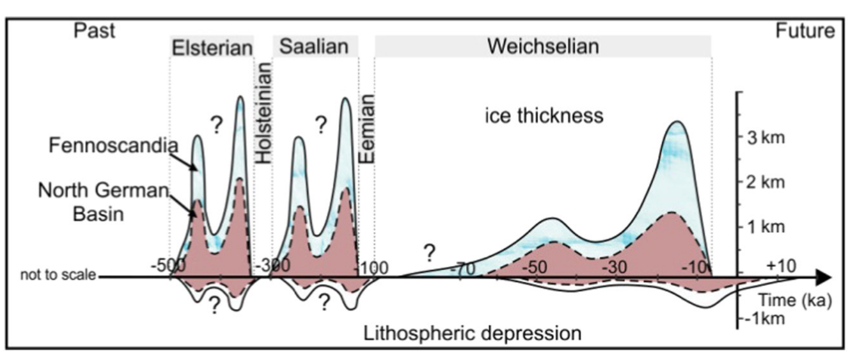

Fig. 25. Relation of the lithospheric depression and ice-loading (modified after Reicherter et al., 2005; Stewart et al., 2000). Note the delay of lithospheric relaxation, which is still lasting in the North German Basin. Weichselian ice thicknesses are after Piotrowski and Tulaczyk (1999) and Elverhøi et al. (1993).

Basin. This assumption is consistent with the analysis of the time-isochore maps of post-Permian strata in the Bays of Kiel and Mecklenburg made by Hansen et al. (2005) and Hübscher et al. (2010). These authors suggested a causative correlation between tectonic evolution of the basin and halokinetics. In contrast to the salt pillows, which emerged above the Triassic fault systems in the Bay of Kiel, the Cenozoic salt movement activity is most pronounced in the Bay of Mecklenburg (Hübscher et al., 2010). Thus, it is a reasonable assumption that the present-day NW-SE directed extension stress field in the region caused faulting of the inherited sub-salt faults triggering diapirism and halokinetics.

These findings may offer possible explanations for recent supra-salt faulting (halokinetics) induced by sub-salt tectonics, such as in Figs. 7, 8 and 12, caused by the current stress field. However, both studies (Hansen et al., 2005; Hübscher et al., 2010) did not discuss the impact of ice sheets on salt structures within the North German Basin.

6.4.3. Ice-loading/unloading and present-day stress field interaction

The present-day stress field in the study area, primarily due to plate motion, is generally directed NW-SE (Kley et al., 2008), while the horizontal stresses acting during the retreating of the Fennoscandia ice sheet would have orientated NE-SW to NNE-SSW (Piotrowski, 1997; Piotrowski and Tulaczyk, 1999). According to Muir-Wood (2000), some destructive interference are expected since these forces are almost moving perpendicular to each other. Accordingly, we suggest that recent tectonics and upward propagation of the faults resulted from differential ice-sheet loading and/or present-day stress field interaction. We also propose that the NW-SE, N-S and NNE-SSW striking faults within the southwest Baltic Sea are optimally orientated of being reactivated as a result of this interaction. This finding may explain why the lateral continuity of reflections between IUC1 and BPU is disturbed to both sides of the faults in Fig. 5.

As stated earlier, the spatial density of shallow faults is much higher in the salt influenced North German Basin compared to the salt free Tornquist Zone. In the salt free Tornquist Zone, two major fault trends are observed: NW-SE and NE-SW striking faults. The majority of these faults are located above basement faults that follow the direction of the Tornquist Zone (Fig. 19). While in the salt influenced North German Basin, the maximum Pleistocene faults show apparent link with the N-S to NNE-SSW striking fault pattern related to the Glückstadt Graben faults. Several of these faults are located directly above basement (sub-salt) faults and salt pillows. The majority of these faults in the Bays of Kiel and Mecklenburg are trending N-S to NNE-SSW and parallel the direction of the Glückstadt Graben faults (Fig. 24). Other Pleistocene faults show coincidence with the NW-SE striking basement fault, such as the Langeland and Prerow Faults (Fig. 1). These observations are in good agreement with Reicherter et al. (2005) interpretation. These authors studied satellite and morphological lineaments in northern Germany and concluded that these features show coincidence with the NW-SE and NNE-SSW striking basement faults therein. Based on our interpretation, we conclude that basement tectonics controls supra-salt tectonics, but the ductile salt layer causes an offset between the sub- and supra-salt faults (Fig. 24).

A correlation between salt structures, glacigenic features and faulting of Pleistocene deposits above salt structures and pre-existing faults has been recognized in many places of the formerly glaciated areas in northern CEBS and attributed to GIA (e.g., Al Hseinat and Hübscher, 2014; Brandes et al., 2015; Brandes and Tanner, 2012; Craig et al., 2016; Lang et al., 2014; Lehné and Sirocko, 2007, 2010; Liszkowski, 1993; Sirocko et al., 2008; Stackebrandt, 2005).

The interactions of ice sheets and salt structures are complex and affected by factors as GIA and the regional stress field on a larger scale and permafrost and subsurface salt dissolution on a more local scale (cf., Grassmann et al., 2010; Lang et al., 2014). These authors discussed various aspects of lateral salt flow and fault reactivation, triggered by ice-load applied onto a salt source layer during the glaciation. Based on high-resolution multi-channel seismic data, Al Hseinat et al. (2016) discussed subsurface faulting and salt tectonics by ice-load induced salt flow and fault reactivation within the southwest Baltic Sea. They suggested a 3D–conceptual model describing reactivation and upward propagation of the supra-salt faults in the Pleistocene.

We suggest that both factors, the ice-sheet loading and/or present-day stress field, may have acted in combination, since faults oriented perpendicular to the orientation of the horizontal stress induced by the deglaciation are believed to have a higher probability of being reactivated (Brandes et al., 2011; Sandersen and Jørgensen, 2015; Stewart et al., 2000).

The number of shallow faults increases further within the salt influenced North German Basin and towards the Glückstadt Graben in the western Bay of Kiel. We therefore explain that the ice-load induced tectonics and/or present-day stress field have a particular strong impact on halokinetics, e.g., caused by supra-salt faulting or salt movement due to ice-load. The latter interpretation has been corroborated by digital models by others (e.g., Lang et al., 2014). Al Hseinat et al. (2016) also pointed out a three phase response of salt structure to ice-sheet loading which depends on the location of the ice margins relative to salt structure during maximum ice advance. If salt structures are affected by faulting due to GIA, salt flow will be triggered (Al Hseinat and Hübscher, 2014) which would add to the deformation of the strata above a salt structure.

Since the Baltic Sea emerged in the Holocene, the findings are not just valid for the marine realm. Most likely, shallow and recently active faults are also present in the hinterland of northern Germany, Poland and southern Denmark. Exogenous processes and anthropogenic activities may have overprinted surface near faults. However, the combination of ice-load induced tectonics and the present-day stress field are good candidates, e.g., for the actual vertical movement of Schleswig-Holstein (Northern Germany) as measured by Lehné and Sirocko (2005, 2007, 2010).

7. Conclusions

- Numerous faults dissect Upper Cretaceous and Tertiary strata in the southwestern Baltic. Several of these faults propagate upwards across the unconsolidated Pleistocene deposits and occasionally pierce the seafloor.
- In the salt influenced North German Basin, most of the faults are approximately located above basement (sub-salt) faults and salt pillows. N-S to NNE-SSW fault trends relate to the Glückstadt Graben and NW-SE trending faults relate to the Tornquist Zone.
- Basement (sub-salt) tectonics controls supra-salt tectonics, but the ductile salt layer causes a lateral shift between the sub- and supra-salt faults.
- In the salt free Tornquist Zone (Pomeranian Bay), the two major trends of the faults are NW-SE and NE-SW. The majority of these faults are located above basement faults and following the trend of the Tornquist Zone.
- Reactivation of inherited faults and vertical salt movement results from major plate reorganisation related to the Late Cretaceous Africa-Iberia-Europe convergence and the subsequent Alpine Orogeny. A later phase of fault reactivation between Late Eocene and Middle Miocene occurred when the principal horizontal stress orientation changed from a NE-SW to a NW-SE direction, which is the present-day orientation.
- Ice-sheet loading and unloading, large-scale glacial isostatic adjustment as well as the present-day stress field combined to cause Late Pleistocene to recent faulting.
- The spatial density of shallow faults is much higher in the salt influenced North German Basin compared to the salt free Tornquist Zone, because ductile salt layers are particular susceptible to ice-load.
- All conclusions are presumably valid for the coastal areas and the hinterland of the marine study area.

Acknowledgements

We thank Editor Rob Govers and anonymous reviewers for their help in improving the manuscript. The authors would like also to thank Holger Lykke-Andersen for providing the BaltSeis data. We would further like to thank Martin Meschede, Karsten Obst and Elisabeth Seidel for fruitful discussions. Per Trinhammer and Sven Winter are thanked for their technical assistant during the data acquisition. The Danish Natural Science Research Council funded the BaltSeis project (grants no. 970176, 9802129 and 9901810). The German Research Foundation funded the NeoBaltic project (DFG grant no. Hu698/7) and later data analysis (DFG grant no. Hu698/21). IHS's and ESRI's are thanked for providing the “KINGDOM” and the “ArcMap” software under an Academic User License Agreement.

References

Al Hseinat, M., Hübscher, C., 2014. Ice-load induced tectonics controlled tunnel valley evolution - instances from the southwestern Baltic Sea. Quat. Sci. Rev. 97, 121–135.

Al Hseinat, M., Hübscher, C., Lang, J., Lüdmann, T., Ott, I., Polom, U., 2016. Triassic to recent tectonic evolution of a crestal collapse graben above a salt-cored anticline in the Glückstadt Graben/North German Basin. Tectonophysics 680, 50–66.

Andren, T., Jorgensen, B.B., Cotterill, C., 2012. Baltic Sea Basin Paleoenvironment: paleoenvironmental evolution of the Baltic Sea Basin through the last glacial cycle. IODP Sci. Prosp. 347. http://dx.doi.org/10.2204/iodp.sp.347.2012.

Arvidsson, R., 1996. Fennoscandian earthquakes: whole crustal rupturing related to postglacial rebound. Science 274, 744–746.

Atzler, R., 1995. The structure of Pleistocene sediments in Kiel Bay and adjacent areas from reflection seismic. Berichte – Reports. Vol. 70. Geologisch-Paläontologisches Institut und Museum Christian-Albrechts-Universität Kiel (pp116).

BABEL Working Group, 1991. Deep seismic survey images the structure of the Tornquist Zone beneath the Southern Baltic Sea. Geophys. Res. Lett. 18, 1091–1094.

BABEL Working Group, 1993. Deep seismic reflection/refraction interpretation of crustal structure along BABEL profiles A and B in the southern Baltic Sea. Geophys. J. Int. 122, 325–343.

Baldschuhn, R., Best, G., Kockel, F., 1991. Inversion tectonics in the North-west German Basin. In: Spencer, A.M. (Ed.), Generation, Accumulation and Production of Europe's Hydrocarbons. Special Publication of the European Association of Petroleum Geoscientists. Vol. 1, pp. 149–159.

Baldschuhn, R., Kockel, F., Best, G., Deneke, E., Frisch, U., Juergens, U., Schmitz, J., Sattler-Kosinowski, S., Stancu-Kristoff, G., Zirngast, M., 1996. Geotektonischer Atlas von NW-Deutschland/Tectonic Atlas of NW-Germany 1:300 000, Vol. Bundesanstalt fuer Geowissenschaften und Rohstoffe, Hannover.

Baldschuhn, R., Binot, F., Fleig, S., Kockel, F., 2001. Geotektonischer Atlas von Nordwest-Deutschland und dem deutschen Nordsee-Sektor. Geologisches Jahrbuch, A 153, 3–95.

Bartholomew, M.J., Stickney, M.C., Wilde, E.M., Dundas, R.G., 2002. Late Quaternary paleoseismites: syndepositional features and section restoration used to indicate paleoseismicity and stress-field orientations during faulting along the main Lima Reservoir fault, southwestern Montana. In: Ettensohn, F.R., Rast, N., Brett, C.E. (Eds.), Ancient Seismites. Geological Society of America, Boulder, Colorado, pp. 29–47 (Special Paper 359).

Bayer, U., Scheck, M., Rabbel, W., Krawczyk, C.M., Götze, H.J., Stiller, M., Beilecke, T., Marotta, A.M., Barrio-Alvers, L., Kuder, J., 1999. An integrated study of the NE-German Basin. Tectonophysics 314, 285–307.

Bergsten, F., 1954. The land uplift in Sweden from the evidence of the old water marks. Geogr. Ann. 36, 81–111.

Berthelsen, A., 1992. From Precambrian to Variscan Europe. In: Blundell, D.J., Freeman, R., Mueller, S. (Eds.), A Continent Revealed – the European Geotraverse. Cambridge University Press, pp. 153–164.

Bowen, D.Q., Rose, J., McCabe, A.M., Sutherland, D.G., 1986. Correlation of Quaternary glaciation in England, Ireland, Scotland and Wales. In: Sibrava, V., Bowen, D.Q., Richmond, G.M. (Eds.), Quaternary Glaciations in the Northern Hemisphere. Quaternary Science Reviews. Vol. 5, pp. 299–340.

Brandes, C., Tanner, D., 2012. Three-dimensional geometry and fabric of shear deformation-bands in unconsolidated Pleistocene sediments. Tectonophysics 518-521, 84–92.

Brandes, C., Polom, U., Winsemann, J., 2011. Reactivation of basement faults: interplay of ice-sheet advance, glacial lake formation and sediment loading. Basin Res. 23, 53–64.

Brandes, C., Pollok, L., Schmidt, C., Wilde, V., Winsemann, J., 2012a. Basin modelling of a lignite-bearing salt rim syncline: insights into rim syncline evolution and salt diapirism in NW Germany. Basin Res. 24, 699–716.

Brandes, C., Winsemann, J., Roskosch, J., Meinsen, J., Tanner, D.C., Frechen, M., Steffen, H., Wu, P., 2012b. Activity of the Osning thrust during the Late Glacial: ice-sheet and lithosphere interactions. Quat. Sci. Rev. 38, 49–62.

Brandes, C., Schmidt, C., Tanner, D.C., Winsemann, J., 2013. Paleostress pattern and salt tectonics within a developing foreland basin (northwestern Subhercynian Basin, northern Germany). Int. J. Earth Sci. 102, 2239–2254.

Brandes, C., Steffen, H., Steffen, R., Wu, P., 2015. Intraplate seismicity in northern Central Europe is induced by the last glaciation. Geology 43, 611–614.

Cameron, T.D.J., Stoker, M.S., Long, D., 1987. The history of Quaternary sedimentation in the UK sector of the North Sea Basin. J. Geol. Soc. Lond. 144, 43–58.

Cartwright, J.A., 1992. The structural evolution of the Ringkøbing-Fyn High. In: Blundell, D.J., Gibbs, A.D. (Eds.), Tectonic Evolution of the North Sea Rifts. Clarendon Press, Oxford, pp. 200–216.

Cathles, L.M., 1975. The Viscosity of the Earth's Mantle. Princeton University Press, Princeton, p. 386.

Clausen, O.R., Huuse, M., 1999. Topography of the Top Chalk surface on- and offshore Denmark. Mar. Pet. Geol. 16, 667–691.

Clausen, O.R., Pedersen, P.K., 1999. The Triassic structural evolution of the southern margin of the Ringkøbing-Fyn High, Denmark. Mar. Pet. Geol. 16, 653–665.

Cloetingh, S., Ziegler, P.A., Beekman, F., Andriessen, P.A.M., Matenco, L., Bada, G., Garcia-Castellanos, D., Hardebol, N., Dèzes, P., Sokoutis, D., 2005. Lithospheric memory, state of stress and rheology: neotectonic controls on Europe's intraplate continental topography. Quat. Sci. Rev. 24, 241–304.

Cocks, L.R.M., McKerrow, W.S., Van Staal, C.R., 1997. The margin of Avalonia. Geol. Mag. 134, 627–636.

Consultants, Gearhart Geo, 1985. Kegnæs-1 well report. Danmark Geologiske Undersøgelser, Denmark, Reportfile No. 9688.

Craig, T.J., Calais, E., Fleitout, L., Bollinger, L., Scotti, O., 2016. Evidence for the release of long-term tectonic strain stored in continental interiors through intraplate earthquakes. Geophys. Res. Lett. 43. http://dx.doi.org/10.1002/2016GL069359.

DEKORP-BASIN Research Group, 1999. Deep crustal structure of the Northeast German basin: new DEKORP-BASIN '96 deep-profiling results. Geology 27 (1), 55–58.

Dong Efterforskning og Production, 2003. Finalwellreport.MAH-1, MAH-1 A (Margretheholm). Technical Report 19622. GEUS, Hørshom.

Dyke, A.S., Morris, T.F., Green, D.E.C., 1991. Postglacial tectonic and sea level history of the central Canadian Arctic. Bull. Geol. Surv. Can. 397.

Ehlers, J., Wingfield, R., 1991. The extension of the Late Weichselian/Late Devensian ice sheets in the North Sea Basin. J. Quat. Sci. 6, 313–326.

Ehlers, J., Grube, A., Stephan, H.-J., Wansa, S., 2011. Pleistocene glaciations of North Germany – new results. In: Ehlers, J., Gibbard, P.L., Hughes, P.D. (Eds.), Quaternary Glaciations – Extent and Chronology – a Closer Look. Developments in Quaternary Science. 15. Elsevier, Amsterdam, pp. 149–162.

Ekman, M., 1991a. A concise history of postglacial land uplift research (from its beginning to 1950). Terra Nova 3, 358–365.

Ekman, M., 1991b. Gravity change, geoid change and remaining postglacial uplift of Fennoscandia. Terra Nova 3, 390–392.

Ekman, M., 2009. The Changing Level of the Baltic Sea during 300 Years: a Clue to Understanding the Earth. Summer Institute for Historical Geophysics, ÃĚland Islands, Sweden (155 pp.).

Ekman, M., Mäkinen, J., 1996. Recent postglacial rebound, gravity change and mantle flow in Fennoscandia. Geophys. J. Int. 126, 229–234.

Elverhøi, A., Fjeldskaar, W., Solheim, A., Nyland-Berg, M., Russwurm, L., 1993. The Barents Sea Ice Sheet—a model of its growth and decay during the last ice maximum. Quat. Sci. Rev. 12, 863–873.

Erlström, M., Thomas, S.A., Deeks, N., Sivhed, U., 1997. Structure and tectonic evolution of the Tornquist Zone and adjacent sedimentary basins in Scania and the southern Baltic Sea area. Tectonophysics 271, 191–215.

EUGENO-S Working Group, 1998. Crustal structure and tectonic evolution of the transition between the Baltic Shield and the North German Caledonides. Tectonophysics 150, 253–348.

von Eynatten, H., Voigt, T., Meier, A., Franzke, H.-J., Gaupp, R., 2008. Provenance of the clastic Cretaceous Subhercynian Basin fill: constraints to exhumation of the Harz Mountains and the timing of inversion tectonics in the Central European Basin. Int. J. Earth Sci. 97, 1315–1330.

Fenton, C., 1994. Postglacial faulting in Eastern Canada. Geological Survey of Canada Open File 2774 (94 pp).

Fisher, M.J., Kockel, F., 1999. Quantification of Early Cimmerian movements in NW-Germany. In: Bachmann, G.H., Lerche, I. (Eds.), Epicontinental Triassic. Zentralblatt für Geologie und Paläontologie, Teil I, pp. 571–600 1998(7–8).

Fisher, M.J., Mudge, D.C., 1998. Triassic. In: Glennie, K.W. (Ed.), Petroleum Geology of the North Sea: Basic Concepts and Recent Advances, fourth ed. Blackwell Science (656pp).

Grad, M., Janik, T., Yliniemi, J., Guterch, A., Luosto, U., Tiira, T., Komminaho, K., Środa, P., Höing, K., Makris, J., Lund, C.E., 1999. Crustal structure of the Mid-Polish Trough beneath the Teisseyre-Tornquist Zone seismic profile. Tectonophysics 314, 145–160.

Grassmann, S., Cramer, B., Delisle, G., Messner, J., Winsemann, J., 2005. Geological history and petroleum system of the Mittelplate oil field, Northern Germany. Int. J. Earth Sci. 94, 979–989.

Grassmann, S., Cramer, B., Delisle, G., Hantschel, T., Messner, J., Winsemann, J., 2010. pT-effects of Pleistocene glacial periods on permafrost, gas hydrate stability zones and reservoir of the Mittelplate oil field, northern Germany. Mar. Pet. Geol. 27, 298–306.

Gregersen, S., Voss, P., TOR Working Group, 2002. Summary of project TOR: delineation of a stepwise, sharp, deep lithosphere transition across Germany – Denmark – Sweden. Tectonophysics 360, 61–73.

Gregersen, S., Glendrup, M., Larsen, T.B., Voss, P., Rasmussen, H.P., 2005. Seismology: neotectonics and structure of the Baltic Shield. Geological Survey of Denmark and Greenland. Bull 7, 25–28.

Guterch, A., Grad, M., Thybo, H., Keller, G.R., POLONAISE Working Group, 1999. POLONAISE '97 – an international seismic experiment between Precambrian and Variscan Europe in Poland. Tectonophysics 314, 101–121.

Hansen, M.B., Lykke Anderson, H., Dehghani, A., Gajewski, D., Hübscher, C., Olesen, M., Reicherter, K., 2005. The Mesozoic - Cenozoic structural framework of the Bay of Kiel area, western Baltic Sea. Int. J. Earth Sci. 94 (5–6), 1070–1082.

Hansen, M.B., Scheck-Wenderoth, M., Hübscher, C., Lykke Andersen, H., Dehghani, A., Hell, B., Gajewski, D., 2007. Basin evolution of the northern part of the Northeast German Basin - insights from a 3D structural model. Tectonophysics 437 (1–4), 1–16.

Hoth, K., Rusbülu, J., Zagora, K., Beer, H., Hartmann, O., 1993. Die tiefen Bohrungen im Zentralabschnitt der Mittel-europäischen Senke – Dokumentation für den Zeitabschnitt 1962–1990. Geowissenschaften 2 (145 pp).

Hübscher, C., Gohl, K., 2014. Reflection/refraction seismology. In: Harff, J., Meschede, M., Petersen, S., Thiede, J. (Eds.), Encyclopedia of Marine Geosciences, (Encyclopedia of Earth Sciences Series). Vol. 1000. Springer, Dordrecht (p., ISBN: 978-94-007-6644-0). 10.1007/978-94-007-6644-0_128-1.

Hübscher, C., Lykke-Andersen, H., Hansen, M.B., Reicherter, K., 2004. Investigating the Structural Evolution of the Western Baltic. EOS Trans. Am. Geophys. Union 85 (12), 115.

Hübscher, C., Hansen, M., Trinanes, S.P., Lykke-Anderson, H., Gajewski, D., 2010. Structure and evolution of the Northeastern German Basin and its transition onto the Baltic Shield. Mar. Pet. Geol. 27, 923–938.

Hughes, A.L., Gyllencreutz, R., Lohne, Ø.S., Mangerud, J., Svendsen, J.I., 2016. The last Eurasian ice sheets–a chronological database and time-slice reconstruction, DATED-1. Boreas 45, 1–45.

Huuse, M., Lykke-Andersen, H., 2000. Over-deepened Quaternary valleys in the eastern Danish North Sea: morphology and origin. Quat. Sci. Rev. 19, 1233–1253.

Johansson, J.M., Davis, J.L., Scherneck, H.-G., Milne, G.A., Vermeer, M., Mitrovica, J.X., Bennett, R.A., Jonsson, B., Elgered, G., Elósegui, P., Koivula, H., Poutanen, M., Rönnäng, B.O., Shapiro, I.I., 2002. Continuous GPS measurements of postglacial adjustment in Fennoscandia 1. Geodetic results. J. Geophys. Res. 107.

Johnston, A.C., 1987. Suppression of earthquakes by large continental ice sheets. Nature 330, 467–469.

Jørgensen, F., Sandersen, P., 2004. Buried and open tunnel valleys in Denmark- erosion beneath multiple ice sheet. Quat. Sci. Rev. 25, 1339–1363.

Kaiser, A., Reicherter, K., Hübscher, C., Gajewski, D., 2005. Variations of the present-day stress field within the North German Basin – insights from thin shell FE-modeling based on residual GPS-velocities. Tectonophysics 397, 66–72.

Kammann, J., Hübscher, C., Boldreel, L.O., Nielsen, L., 2016. High-resolution shear-wave seismics across the Carlsberg Fault zone south of Copenhagen - implications for linking Mesozoic and late Pleistocene structures. Tectonophysics 682, 56–64.

Kaufmann, G., Wolf, D., 1999. Effects of lateral viscosity variations on postglacial rebound: an analytical approach. Geophys. J. Int. 137 (2), 489–500.

Kierulf, H.P., Steffen, H., Simpson, M.J.R., Lidberg, M., Wu, P., Wang, H., 2014. A GPS velocity field for Fennoscandia and a consistent comparison to glacial isostatic adjustment models. J. Geophys. Res. 119.

Klemann, V., Wolf, D., 2005. The eustatic reduction of shoreline diagrams: implications for the inference of relaxation-rate spectra and the viscosity stratification below Fennoscandia. Geophys. J. Int. 162 (1), 249–256.

Kley, J., Voigt, T., 2008. Late Cretaceous intraplate thrusting in central Europe: effect of Africa-Iberia-Europe convergence, not Alpine collision. Geology 36 (11), 839–842.

Kley, J., Franzke, H.J., Jähne, F., Krawczyk, C., Lohr, T., Reicherter, K., Scheck-Wenderoth, M., Sippe, J., Tanner, D., van Gent, H., the SPP Structural Geology Group, 2008. Strain and stress (Chapter 3.3). In: Littke, R., Bayer, U., Gajewski, D., Nelskamp, S. (Eds.), Dynamics of Complex Intercontinental Basins- the Central European Basin System. Springer-Verlag, Berlin-Heidelberg, pp. 234–245 (ISBN: 978-3-540-85084-7).

Kockel, F., 2003. Inversion structures in Central Europe - expressions and reasons, an open discussion. Neth. J. Geosci. 82 (4), 367–382.

Kossow, D., Krawczyk, C.M., 2002. Structure and quantification of processes controlling the evolution of the inverted NE-German Basin. Mar. Pet. Geol. 19, 601–618.

Kossow, D., Krawczyk, C., McCann, T., Strecker, M., Negendank, J.F.W., 2000. Style and evolution of salt pillows and related structures in the northern part of the Northeast German Basin. Int. J. Earth Sci. 89, 652–664.

Krauss, M., 1994. The tectonic structure below the southern Baltic Sea and its evolution. Z. Geol. Wiss. 22, 19–32.

Krauss, M., Mayer, P., 2004. The Vorpommern fault system and its regional structural relationships to the Trans-European Fault. Z. Geol. Wiss. 32 (2–4), 227–246.

Krawczyk, C.M., Stiller, M., DEKORP-BASIN Research Group, 1999. Reflection seismic constraints on Paleozoic crustal structure and Moho beneath the NE German Basin. Tectonophysics 314, 241–253.

Krawczyk, C.M., Eilts, F., Lassen, A., Thybo, H., 2002. Seismic evidence of Caledonian deformed crust and uppermost mantle structures in the northern part of the Trans-European Suture Zone, SW Baltic Sea. Tectonophysics 360, 215–244.

Krzywiec, P., Kramarska, R., Zientara, P., 2003. Strike-slip tectonics within the SW Baltic Sea and its relationship to the inversion of the Mid-Polish Trough – evidence from high resolution seismic data. Tectonophysics 373, 93–105.

Kujansuu, R., 1964. NuoristasiirroksistaLappissa. Summary: recent faults in Lapland. Andean Geol. 16, 30–36.

Kumar, A., Sunil Singh, L., 2012. Is isostatic Rebound in slow spreading Gakkel Ridge of Artic region due to the climate change? A case study. Int. J. Geosci. 3, 339–348.

Lagerbäck, R., 1978. Neotectonic structures in northern Sweden. Geologiska Föreningen i Stockholm Förhan-dlingar 100, 263–269.

Lagerbäck, R., Sundh, M., 2008. Early Holocene faulting and paleoseismicity in northern Sweden. Sverigesgeologiskaundersökning - Research Paper. Vol. 836.

Lambeck, K., Smither, C., Ekman, M., 1998a. Tests of glacial rebound models for Fennoscandia based on instrumented sea- and lake-level records. Geophys. J. Int. 135, 375–387.

Lang, J., Hampel, A., Brandes, C., Winsemann, J., 2014. Response of salt structures to ice-sheet loading: implications for ice-marginal and subglacial processes. Quat. Sci. Rev. 101, 217–233.

Le Meur, E., 1996. Isostatic postglacial rebound over Fennoscandia with a self-gravitating spherical visco-elastic Earth Model. Ann. Glaciol. 23, 318–327.

Lehné, J., Sirocko, F., 2005. Quantification of recent movement potentials in Schleswig-Holstein (Germany) by GIS-based calculation of correlation coefficients. Int. J. Earth Sci. 94, 1094–1102.

Lehné, R., Sirocko, F., 2007. Rezente Bodenbewegungspotenziale in Schleswig-Holstein (Deutschland) – Ursachen und ihr Einfluss auf die Entwicklung der rezenten Topographie. Z. Dtsch. Ges. Geowiss. 158, 329–347.

Lehné, J., Sirocko, F., 2010. Recent vertical crustal movements and resulting surface deformation within the North German Basin (Schleswig-Holstein) derived by GIS-based analysis of repeated precise leveling data. Z. Dtsch. Ges. Geowiss. 175–188.

Lemke, W., Kuijpers, A., Hoffmann, G., Milkert, D., Atzler, R., 1994. The Darß Sill, hydrographic threshold in the southwestern Baltic. Late Quaternary geology and recent sediment dynamics. Cont. Shelf Res. 14 (7/8), 847–870.

Liboriussen, J., Ashton, P., Tygesen, T., 1987. The tectonic evolution of the Fennoscandian Border Zone in Denmark. Tectonophysics 137, 21–29.

Liszkowski, J., 1993. The effects of Pleistocene ice-sheet loading-deloading cycles on the bedrock structure of Poland. Folia Quat 64, 7–23.

Lokhorst, A., Adlam, K., Brugge, J.V.M., David, P., Diapari, L., Fermont, W.J.J., Geluk, M., Gerling, P., Heckers, J., Kockel, F., Kotarba, M., Laier, T., Lott, G.K., Milaczewski, E., Milaczewski, L., Nicholson, R.A., Von Planten, F., Pokorski, J., 1998. NW European Gas Atlas-Composition and Isotope Ratios of Natural Gases. Netherlands Instituutvoor Toegepaste geowetenschappen, Panstwowy Instytut Geologiczny, European Union.

Long, D., Laban, C., Streif, H., Cameron, T.D.J., Schuttenhelm, R.T.E., 1988. The sedimentary record of Quaternary climatic variations in the southern North Sea. Philos. Trans. R. Soc. Lond. B 318, 523–537.

Ludwig, A.O., 1995. The surface of the Holsteinian interglacial sediments as a base level for reconstruction of vertical neotectonic movements in northern Germany. GeosynoptikaGeoterm 3, 31–36.

Lykke-Andersen, H., Surlyk, F., 2004. The Cretaceous-Paleogene boundary at StevnsKlint, Denmark: inversion tectonics or seafloor topography? J. Geol. Soc. Lond. 161, 343–352.

Lykke-Andersen, H., Seidenkrantz, M.S., Knudsen, K.L., 1993. Quaternary sequences and their relations to the pre-Quaternary in the vicinity of Anholt, Kattegat, Scandinavia. Boreas 22, 291–298.

Maystrenko, Y., Bayer, U., Scheck-Wenderoth, M., 2005a. The Glückstadt Graben, a sedimentary record between the North and Baltic Sea in north Central Europe. Tectonophysics 397 (1–2), 113–126.

Maystrenko, Y., Bayer, U., Brink, H.-J., Littke, R., 2008. The Central European basin system - an overview. In: Littke, R., Bayer, U., Gajewski, D., Nelskamp, S. (Eds.), Dynamics of Complex Sedimentary Basins. The Example of the Central European Basin System. Springer-Verlag, Berlin-Heidelberg, pp. 15–34.

Maystrenko, Y., Bayer, U., Scheck-Wenderoth, M., 2011. 3D structural model of the Glückstadt Graben, NW Germany Scientific Technical Report STR11/08 – data. Potsdam (29 pp).

Meissner, R., Krawczyk, C.M., 1999. Caledonian and Proterozoic terrane accretion in the southwest Baltic Sea. Tectonophysics 314, 255–267.

Mitrovica, J.X., 1996. Haskell [1935] revisited. J. Geophys. Res. 101, 555–569.

Mörner, N.-A., 1979. The Fennoscandian uplift and late Cenozoic geodynamics: geological evidence. GeoJournal 3 (3), 287–318.

Muir-Wood, R., 2000. Deglaciation Seismotectonics: a principal influence on intraplate seismogenesis at high latitudes. Quat. Sci. Rev. 19, 1399–1411.

Munier, R., Fenton, C., 2004. Review of postglacial faulting - current understanding and directions for future studies. Respect Distances - Rationale and Means of Computation. Swedish Nuclear Fuel and Waste Management Co., Stockholm (Report R-04-17, 62 pp).

NIA-Netherlands Institute of Applied Geoscience TNO, 2000. Northwestern European Gas Atlas, Published on CD-ROM, Utrecht.

Nielsen, L.H., Japsen, P., 1991. Deep Wells in Denmark 1935–1990 – Lithostratigraphic Subdivision. Danmarks Geologiske Undersøgelser, Denmark (223pp).

Olesen, O., 1988. The Stuoragurra Fault, evidence of neotectonics in the Precambrian of Finnmark, northern Norway. Nor. Geol. Tidsskr. 68, 107–118.

Pasierbski, M., 1979. Remarks on the genesis of sub-glacial channels in Northern Poland. Eiszeit. Gegenw. 29, 189–200.

Pharaoh, T.C., England, R.W., Verniers, J., Zelazniewicz, A., 1997. Introduction: geological and geophysical studies in the trans-European Suture Zone. Geol. Mag. 134, 585–590.

Piotrowski, J.A., 1997. Subglacial hydrology in north-western Germany during the last glaciation: groundwater flow, tunnel valleys and hydrological cycles. Quat. Sci. Rev. 162, 169–185.

Piotrowski, J.A., Tulaczyk, S., 1999. Subglacial conditions under the last ice sheet in northwest Germany: ice bed separation and enhanced basal sliding Germany? Quat. Sci. Rev. 18, 737–751.

Plag, H.-P., Engen, B., Clark, T.A., Degnan, J.J., Richter, B., 1998. Post-glacial rebound and present-day three-dimensional deformations. J. Geodyn. 25 (3/4), 263–301.

Pokorski, J., 1990. Rotliegendes in the nortwesternmost Pomerania and the adjacent Baltic Basin (in Polish with English summary). Kwartalnik Geol. 34 (1), 79–92.

Quinlan, G., 1984. Postglacial rebound and the focal mechanisms of eastern Canadian earthquakes. Can. J. Earth Sci. 21, 1018–1023.

Reicherter, K., Kaiser, A., Stackebrandt, W., 2005. The post-glacial landscape evolution of the North German Basin: morphology, neotectonics, and crustal deformation. Int. J. Earth Sci. 94, 1083–1093.

Reicherter, K., Froitzheim, N., Jarosiski, Badura, J., Franzke, H.-J., Hansen, M.B., Hübscher, C., Müller, R., Poprawa, P., Reinecker, J., Stackebrandt, W., Voigt, H., von Eynatten, H., Zuchiewicz, W., 2008. Alpine tectonics north of the Alps. In: McCann, T. (Ed.), Geology of Central Europe. Special Publication. Geological Society, London.

Roskosch, J., Winsemann, J., Polom, U., Brandes, C., Tsukamoto, S., Weitkamp, A., Bartholomäus, W.A., Henningsen, D., Frechen, M., 2015. Luminescence dating of ice-marginal deposits in northern Germany: evidence for repeated glaciations during the Middle Pleistocene (MIS 12 to MIS 6). Boreas 44, 103–126.

Roth, F., Fleckenstein, P., 2001. Stress orientation found in northeast Germany differ from the West European trend. Terra Nova 13, 289–296.

Salomonsen, I., 1993. Quaternary buried valley systems in the eastern North Sea. Ph.D Thesis. University of Copenhagen.
Salomonsen, I., 1995. Origin of a deep buried valley system in Pleistocene deposits of the eastern central North Sea. In: Michelsen, O. (Ed.), Proceedings of the Second Symposium on: Marine Geology-Geology of the North Sea and Skagerrak Geological Survey of Denmark, Series C. Vol. 12, pp. 7–19.
Sandersen, P., Jørgensen, F., 1998. Kortlvgning af begravede dalsystemer i Jylland - et forprojekt. Det jyske grundvandssamarbejde. Watertech A/S, Vejle Amt (unpublished report).
Sandersen, P.B.E., Jørgensen, F., 2015. Neotectonic deformation of a Late Weichselian outwash plain by deglaciation-induced fault reactivation of a deep-seated graben structure. Boreas 44 (2), 413–431.
Sauber, J., Molnia, B., 2004. Glacier ice mass fluctuations and fault instability in tectonically active southern Alaska. Glob. Planet. Chang. 42, 279–293.
Scheck, M., Bayer, U., 1999. Evolution of the Northeast German Basin—inferences from 3D structural modelling and subsidence analysis. Tectonophysics 313, 145–169.
Scheck, M., Bayer, U., Lewerenz, B., 2003a. Salt movements in the Northeast German Basin and its relation to major post-Permian tectonic phases-results from 3D structural modelling, backstripping and reflection seismic data. Tectonophysics 361, 277–299.
Scheck, M., Bayer, U., Lewerenz, B., 2003b. Salt redistribution during extension and inversion inferred from 3D backstripping. Tectonophysics 373, 55–73.
Scheck-Wenderoth, M., Lamarche, J., 2005. Crustal memory and basin evolution in the Central European Basin System – new insights from a 3D structural model. Tectonophysics 397, 143–165.
Schlüter, H.U., Best, G., Jürgens, U., Binot, F., 1997. Interpretation reflexionsseismischer profile zwischen baltischer kontinentalplattes und kaledonisches Becken in der südlichen ostsee-erste Ergebnisse. Z. Dtsch. Geol. Ges. 148 (1), 1–32.
Schlüter, H.U., Jürgens, U., Binot, F., Best, G., 1998. The importance of geological structures as natural sources of potentially hazardous substances in the southern part of the Baltic Sea. Z. Dtsch. Geol. Ges. 44 (1).
Schwarz, C., 1996. Neue Befunde zur Verbreitung und Dimension pleistozäner Rinnensysteme auf dem deutschen Nordseeschelf. Geol. Jahrb. 146, 233–244.
Seifert, T., Tauber, F., Kayser, B., 2001. A high resolution spherical grid topography of the Baltic Sea - 2nd edition. Baltic Sea Science Congress, Stockholm, 2529 November 2001, Poster# 147 (In: www.io-warnemuende.de/iowtopo).
Shilts, W.W., Rappol, M., Blais, A., 1992. Evidence of late and postglacial seismic activity in the Témiscouata-Madawaska Valley, Quebec - New Brunswick, Canada. Can. J. Earth Sci. 29, 1043–1059.
Shomali, Z.H., Roberts, R.G., Pedersen, L.B., TOR Working Group, 2006. Lithospheric structure of the Tornquist Zone resolved by nonlinear P and S teleseismic tomography along the TOR array. Tectonophysics 416, 133–149.
Sirocko, F., Reicherter, K., Lehne, R., Hübscher, Ch., Winsemann, J., Stackebrandt, W., 2008. Glaciation, salt and the present landscape (Chapter 4.5). In: Littke, R., Bayer, U., Gajewski, D., Nelskamp, S. (Eds.), Dynamics of Complex Intercontinental Basins - The Central European Basin System. Springer-Verlag, Berlin-Heidelberg, pp. 234–245 (ISBN: 978-3-540-85084-7).
Smit, J., van Wees, Jan-Diederik, Cloetingh, S., 2016. The Thor suture zone: from subduction to intraplate basin setting. Geology 44 (9), 707–710.
Spada, G., Barletta, V.R., Klemann, V., Riva, R.E.M., Martinec, Z., Gasperini, P., Lund, B., Wolf, D., Vermeersen, L.L.A., King, M.A., 2011. A benchmark study for glacial isostatic adjustment codes. Geophys. J. Int. 185 (1), 106–132.
Stackebrandt, W., 1986. Beiträge zur tektonischen Analyse ausgewählter Bruchzonen der Subherzynen Senke und angrenzender Gebiete (Aufrichtungszone, Flechtinger Scholle). Veröff Zentralinst. Phys. Erde 79 (79 pp.).
Stackebrandt, W., 2005. Neotektonische Aktivitätsgebiete in Brandenburg (Norddeutschland). Brandenburgische Geowissenschaftliche Beiträge 12, 165–172.
Steffen, H., Wu, P., 2011. Glacial isostatic adjustment in Fennoscandia - a review of data and modeling. J. Geodyn. 52, 169–204.
Steffen, H., Kaufmann, G., Wu, P., 2006. Three-dimensional finite-element modelling of the glacial isostatic adjustment in Fennoscandia. Earth Planet. Sci. Lett. 250, 358–375.
Steffen, R., Steffen, H., Wu, P., Eaton, D.W., 2014a. Stress and fault parameters affecting fault slip magnitude and activation time during a glacial cycle. Tectonics 33 (7), 1461–1476.
Steffen, R., Wu, P., Steffen, H., Eaton, D.W., 2014b. On the implementation of faults in finite-element glacial isostatic adjustment models. Comput. Geosci. 62, 150–159.
Steffen, R., Wu, P., Steffen, H., Eaton, D.W., 2014c. The effect of earth rheology and ice-sheet size on fault slip and magnitude of postglacial earthquakes. Earth Planet. Sci. Lett. 388, 71–80.
Steffen, R., Steffen, H., Wu, P., 2016. Comparison of the glacial isostatic adjustment behaviour in glacially induced fault models. Geosci. Model Dev. 9, 1153–1200.
Stewart, Is, Sauber, J., Rose, J., 2000. Glacio-seismotectonics: ice sheets, crustal deformation and seismicity. Quat. Sci. Rev. 19, 1367–1389.
Taylor, J.C.M., 1998. Upper Permian – Zechstein. In: Glennie, K.W. (Ed.), Petroleum Geology of the North Sea: Basic Concepts and Recent Advances, fourth ed. Blackwell Science (656 pp.).
Thomas, S., Sivhed, U., Erlström, M., Seifert, M., 1993. Seismostratigraphy and structural framework of the SW Baltic Sea. Terra Nova 5, 364–374.
Thybo, H., 2001. Crustal structure along the EGT profile across the Tornquist Fan interpreted from seismic, gravity and magnetic data. Tectonophysics 334, 155–190.
Turpeinen, H., Hampel, A., Karow, T., Maniatis, G., 2008. Effect of ice sheet growth and melting on the slip evolution of thrust faults. Earth Planet. Sci. Lett. 269 (1–2): 230–241. http://dx.doi.org/10.1016/j.epsl.2008.02.017.
Underhill, J.R., 1998. Jurassic. In: Glennie, K.W. (Ed.), Introduction to the Petroleum Geology of the North Sea. Vol. 656. Blackwell Science, pp. 245–293.
Vejbæk, O.V., 1985. Seismic Stratigraphy and tectonics of Sedimentary Basins around Bornholm, southern Baltic. Danmarks. Geologiske Undersøgelser for Danmark 8, 1–29.
Vejbæk, O.V., 1997. Dype strukturer I danske sedimentære bassiner. Gelogisk Tidsskrift 4, 1–31.
Voigt, T., Wiese, F., von Eynatten, H., Franzke, H.-J., Gaupp, R., 2006. Facies evolution of syntectonic Upper Cretaceous deposits in the Subhercynian Cretaceous Basin and adjoining areas (Germany). Z. Dtsch. Ges. Geowiss. 157, 203–244.
van Wees, J.D., Stephenson, R.A., Ziegler, P.A., Bayer, U., McCann, T., Dadlez, R., Gaupp, R., Narkiewicz, M., Bitzer, F., Scheck, M., 2000. On the origin of the Southern Permian Basin, Central Europe. Mar. Pet. Geol. 17, 43–59.
Whitehouse, P., 2009. Glacial Isostatic Adjustment and Sea-level Change: State of the Art Report. TR-09-11. Kärnbränslehantering AB, Svensk.
Wolf, D., 1993. The changing role of the lithosphere in models of glacial isostasy: a historical review. Glob. Planet. Chang. 8, 95–106.
Wu, P., van der Wal, W., 2003. Postglacial sea levels on a spherical, self-gravitating visco-elastic earth: effects of lateral viscosity variations in the upper mantle on the inference of viscosity contrasts in the lower mantle. Earth Planet. Sci. Lett. 211, 57–68.
Wu, P., Johnston, P., Lambeck, K., 1999. Postglacial rebound and fault instability in Fennoscandia. Geophys. J. Int. 139, 657–670.
Ziegler, P.A., 1990. Geological Atlas of Western and Central Europe. second ed. Shell International Petroleum Maatschappij BV, distributed by Geological Society Publishing House (239 pp).
Zöllner, H., Reicherter, K., Schikowsky, P., 2008. High-resolution seismic analysis of the coastal Mecklenburg Bay (North German Basin): the pre-Alpine evolution. Int. J. Earth Sci. 97 (5), 1013–1027.